CAPITAL UNIVERSITY OF SCIENCE AND TECHNOLOGY, ISLAMABAD

Automation of Bonnet Polishing System Using Deep Feature Fusion and K-Means-Based Data Segmentation

by

Aitzaz Ahmed Murtaza

A thesis submitted in partial fulfillment for the degree of Master of Science

in the

Faculty of Engineering
Department of Mechanical Engineering

2025

Copyright © 2025 by Aitzaz Ahmed Murtaza

All rights reserved. No part of this thesis may be reproduced, distributed, or transmitted in any form or by any means, including photocopying, recording, or other electronic or mechanical methods, by any information storage and retrieval system without the prior written permission of the author.

This thesis is dedicated to all those who have stood by me throughout this journey — to my family, for their endless love and sacrifices, to my mentors, for their guidance and belief in my potential, and to my friends, for their support and encouragement in moments of doubt.
Your presence has made this achievement possible.

CERTIFICATE OF APPROVAL

Automation of Bonnet Polishing System Using Deep Feature Fusion and K-Means-Based Data Segmentation

by

Aitzaz Ahmed Murtaza

(MME233001)

THESIS EXAMINING COMMITTEE

S. No.	Examiner	Name	Organization
(a)	External Examiner	Dr. Muhammad Jawad Khan	NUST, Islamabad
(b)	Internal Examiner	Dr. Imtiaz Ahmad Taj	CUST, Islamabad
(c)	Supervisor	Dr. Shummaila Rasheed	CUST, Islamabad

Dr. Shummaila Rasheed
Thesis Supervisor
September, 2025

Dr. Mahabat Khan
Head
Dept. of Mechanical Engineering
September, 2025

Dr. Imtiaz Ahmad Taj
Dean
Faculty of Engineering
September, 2025

Author's Declaration

I, **Aitzaz Ahmed Murtaza** hereby state that my MS thesis titled "**Automation of Bonnet Polishing System Using Deep Feature Fusion and K-Means-Based Data Segmentation**" is my own work and has not been submitted previously by me for taking any degree from Capital University of Science and Technology, Islamabad or anywhere else in the country/abroad.

At any time if my statement is found to be incorrect even after my graduation, the University has the right to withdraw my MS Degree.

(Aitzaz Ahmed Murtaza)
Registration No: MME233001

Plagiarism Undertaking

I solemnly declare that research work presented in this thesis titled "**Automation of Bonnet Polishing System Using Deep Feature Fusion and K-Means-Based Data Segmentation**" is solely my research work with no significant contribution from any other person. Small contribution/help wherever taken has been duly acknowledged and that complete thesis has been written by me.

I understand the zero tolerance policy of the HEC and Capital University of Science and Technology towards plagiarism. Therefore, I as an author of the above titled thesis declare that no portion of my thesis has been plagiarized and any material used as reference is properly referred/cited.

I undertake that if I am found guilty of any formal plagiarism in the above titled thesis even after award of MS Degree, the University reserves the right to withdraw/revoke my MS degree and that HEC and the University have the right to publish my name on the HEC/University website on which names of students are placed who submitted plagiarized work.

(Aitzaz Ahmed Murtaza)
Registration No: MME233001

Acknowledgement

I would first like to express my deepest gratitude to Dr. Shummaila Rasheed, my supervisor, for her continuous encouragement, insightful guidance, and unwavering support throughout the course of this research. Her mentorship provided the foundation on which this work was built, and her belief in my potential kept me motivated and focused.

I am especially thankful to Dr. Muhammad Faisal Aftab from the Department of Engineering Sciences, University of Agder, Grimstad, Norway, for conceptualizing this research direction and providing technical insights that helped shape the core methodology. His vision and input were instrumental in aligning this work with modern research goals in intelligent manufacturing.

My sincere appreciation goes to my friend, Muhammad Hamza Zafar, for his invaluable technical assistance and academic support not only during this project but throughout my entire master's journey. His collaborative spirit, reliability, and continuous encouragement made a truly meaningful difference.

Finally, I am thankful to my family and friends whose support and motivation carried me through the most challenging phases of this journey. In particular, I extend my heartfelt gratitude to my wife, Amna Saher, whose unwavering encouragement, patience, and belief in me have been a source of constant strength throughout this academic pursuit.

(Aitzaz Ahmed Murtaza)

Abstract

Polishing plays a vital role in fabricating high-precision optical components, where accurate control of the Material Removal Rate (MRR) is critical. Traditional MRR estimation methods rely on surface profilometry before and after, which is time consuming and unsuitable for real-time process control. This work presents a machine learning-based framework for near real-time MRR prediction using in-process sensor signals collected during bonnet polishing. The proposed approach begins with automated segmentation of polishing and non-polishing data regions using K-means clustering, replacing the need for manual data trimming. A hybrid feature extraction pipeline follows: time-averaged statistical features are processed through an Artificial Neural Network (ANN) branch, while a Multi-Branch Attention Residual CNN (MARCNN) handles time-domain, frequency-domain, and wavelet-transformed features derived from force sensor data. The dense features from these two branches are then fused together for accurate regression.

The deep feature fusion network achieved high accuracy, with a Mean Absolute Error (MAE) of 0.0563 µm and an R^2 score of 0.9881, demonstrating its ability to generalize across varying polishing conditions. Explainability analysis using SHAP and Grad-CAM showed that vertical (normal) and lateral (frictional) force components were the most influential in predicting MRR. Ablation studies revealed that adding slurry pH and temperature features resulted in marginal performance gains, suggesting the dominance of force-based features. Overall, this work presents a robust and interpretable framework capable of supporting adaptive control strategies in ultra-precision polishing processes.

Contents

List of Figures

List of Tables

Abbreviations

ANN	Artificial Neural Network
DWT	Discrete Wavelet Transform
FD	Frequency-Domain
Grad-CAM	Gradient-weighted Class Activation Mapping
MARCNN	Multi-branch Attention Residual Convolutional Neural Network
MRR	Material Removal Rate
SHAP	SHapley Additive exPlanations
TD	Time-Domain

Symbols

k	Preston's coefficient	µm/(N·mm/min)
p	Applied pressure	N/mm^2
v	Relative velocity between tool and surface	mm/min
y_i	Ground truth MRR value for sample i	μm
$\hat{y}_i$	Predicted MRR value for sample i	μm
u_{Aj}	Mean of approximation coefficients from DWT	Unitless
A_j	Approximation coefficients in DWT decomposition	Unitless
P_k	Power spectral component at frequency bin k	Unitless
H	Spectral entropy of the signal	Unitless
E	Total spectral energy of the signal	Unitless

Chapter 1

Introduction, Problem Framing, and Research Objectives

In the realm of modern manufacturing, the demand for high-precision components with exceptional surface quality is continually increasing. Whether in optics, aerospace, semiconductor devices, or biomedical implants, surface finish plays a critical role in determining the functionality, efficiency, and reliability of a product [1]. To meet such demanding requirements, various surface finishing techniques have been developed, among which polishing is one of the most widely used processes for achieving micro- and nano-level surface smoothness.

Polishing, by definition, is a material removal process that enhances the surface quality of a workpiece by eliminating surface irregularities through mechanical, chemical, or a combination of actions. It is typically performed after grinding or machining operations to improve dimensional accuracy and reduce surface roughness [2]. The process is essential not only for aesthetic purposes but also for ensuring the proper mechanical and optical performance of precision components.

With the advancement of manufacturing technologies, there has been a growing emphasis on automating traditional processes to increase consistency, reduce dependence on manual labour, and enhance overall efficiency. However, polishing

particularly for complex geometries remains a challenging process to automate due to its reliance on operator skill and its sensitivity to process parameters.

Among the various polishing methods, bonnet polishing has emerged as a promising candidate for automation due to its adaptable, controlled material removal capabilities and its suitability for free-form surfaces. In this context, the integration of machine learning (ML) techniques into the polishing process offers new opportunities for intelligent automation. ML can be used to model the complex relationships between polishing parameters and outcomes, such as the Material Removal Rate (MRR), enabling data-driven control and optimization of the process. Accurate prediction of MRR is essential for planning, monitoring, and automating the polishing operation, especially when dealing with variable materials and component geometries.

This thesis explores the automation of the bonnet polishing process by employing machine learning models to predict the MRR. By combining domain knowledge in manufacturing with the predictive power of ML algorithms, the objective is to build a system that not only improves the reliability of MRR estimation but also enables closed-loop control for fully or semi-automated polishing systems.

1.1 What is Polishing?

Polishing is a surface finishing process used to improve the smoothness, reflectivity, and dimensional accuracy of a material by removing a thin layer from its surface [3]. It is typically employed in the final stages of manufacturing to eliminate surface imperfections such as scratches, pits, tool marks, or residual stress introduced by previous machining operations.

The ultimate goal of polishing is to achieve a mirror-like finish or a surface roughness that meets stringent functional and aesthetic requirements. Unlike abrasive machining processes such as grinding, which are primarily focused on material removal for shaping, polishing operates at a much finer scale, often in the micrometer or nanometre range [4].

The process generally involves the use of abrasive particles, suspended in a polishing slurry or embedded in a flexible polishing pad, which are brought into controlled contact with the surface under specific pressure and relative motion [5].

Polishing is used in a wide variety of industries:

- In optics, it ensures precise surface curvature and clarity for lenses and mirrors [2].
- In semiconductor manufacturing, it is critical for wafer planarization and defect elimination [6].
- In biomedical and aerospace applications, it ensures biocompatibility and aerodynamic performance, respectively [7, 8].
- In automotive and decorative industries, it improves surface lustre and visual appeal [9].

The effectiveness of a polishing process depends on various parameters. The type and size of the abrasive material determine the rate and smoothness of material removal. The geometry of the tool affects the contact area and the uniformity of the material removal.

Similarly, the contact pressure determines the depth and rate of material removal. Relative speed controls the interaction dynamics between the tool and surface. Polishing time and path determines the uniformity and depth of polish [10]. Despite its widespread use, polishing remains a complex and often empirically-driven process, with many variables interacting in non-linear ways.

Achieving consistent results, especially on complex or free-form surfaces, requires significant expertise, and this challenge has led to increased interest in automating and optimizing the process through intelligent control systems, including machine learning.

1.2 Types of Polishing Techniques

Over the years, a variety of polishing techniques have been developed to meet the specific needs of different materials, surface geometries, and application domains. These techniques differ in their mechanisms of material removal, tool design, and degree of control. Understanding these methods is essential to appreciate the unique advantages of bonnet polishing and its potential for automation.

1.2.1 Manual Polishing

Manual polishing is one of the oldest and most basic surface finishing techniques, traditionally performed by skilled operators using abrasive papers, cloths, or pastes as illustrated in Fig. 1.1. The material is removed from the surface through direct physical contact, where the abrasive particles embedded in the medium gradually wear down the irregularities of the surface. Although simple in setup and cost-effective for small-scale tasks, the technique relies heavily on the experience and consistency of the operator. The pressure applied, duration of polishing, and motion patterns are all manually controlled, leading to high variability in outcomes. As a result, manual polishing lacks repeatability and precision, making it unsuitable for high-accuracy or high-volume manufacturing environments [11].

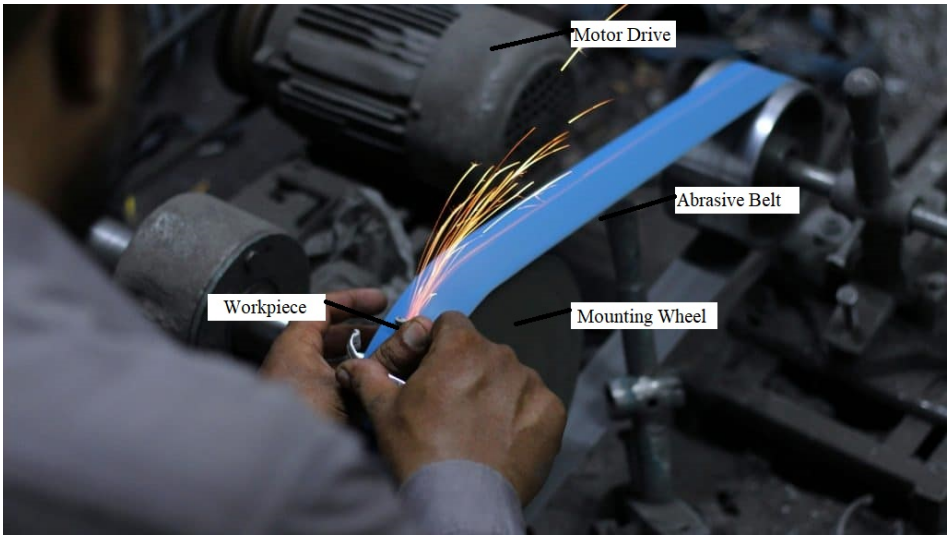

FIGURE 1.1: A worker polishing a workpiece on an abrasive belt polishing machine.

Despite these limitations, manual polishing is still employed in applications such as prototyping, reworking, or artistic finishing, where tactile feedback and visual inspection play a role. However, it poses challenges when uniform surface quality, high geometrical precision, and controlled material removal rates (MRR) are required. The absence of quantitative feedback mechanisms and process automation also makes it difficult to monitor or adjust polishing parameters in real time [12]. Consequently, manual polishing has been largely replaced in precision industries by more deterministic and automated polishing methods that offer better control, consistency, and integration with modern process monitoring tools.

1.2.2 Chemical Mechanical Polishing (CMP)

CMP is a widely adopted planarization technique, especially in the semiconductor and optics industries, where nano-metric surface smoothness and global flatness are critical. CMP synergistically combines chemical and mechanical forces to achieve material removal through the simultaneous action of a reactive slurry and mechanical abrasion. The process involves a rotating polishing pad wetted with a chemically active slurry that reacts with the workpiece surface. Meanwhile, mechanical force applied via a polishing head ensures the continual removal of the reacted surface layer. The interplay of chemical etching and mechanical abrasion enables CMP to achieve both high precision and excellent surface quality, making it a cornerstone technique in integrated circuit (IC) fabrication and high-end optics finishing [13].

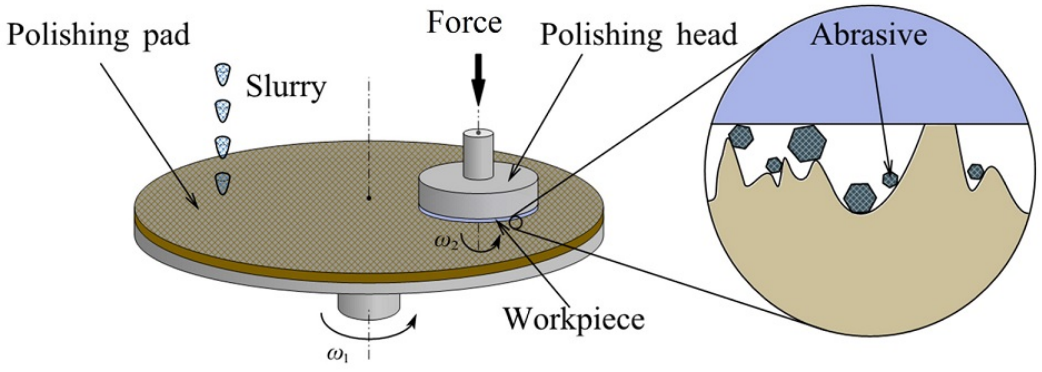

FIGURE 1.2: Schematic illustration of the CMP process. Source: [14]

The general schematic of a CMP setup is shown in Fig. 1.2, showing the interaction between the rotating wafer, the slurry, and the polishing pad. This configuration ensures a uniform pressure distribution and controlled material removal across the surface. Key parameters such as downforce pressure, pad rotation speed, and slurry composition must be fine-tuned to maintain process stability and surface integrity.

Although CMP is capable of atomic-level precision, it requires sophisticated end-point detection and process control strategies because of its sensitivity to pad wear, slurry dynamics, and chemical reactions. However, CMP remains an indispensable polishing method for applications requiring extremely tight planarization tolerances.

1.2.3 Magnetorheological Polishing (MRP)

MRP is an advanced ultra-precision surface finishing technique that utilizes the unique rheological properties of magnetorheological fluids to achieve controlled material removal. These fluids, typically composed of iron particles suspended in a carrier liquid along with abrasive particles, change viscosity when subjected to a magnetic field.

In the MRP process, a rotating polishing tool or belt introduces the magnetorheological fluid into a polishing zone while a magnetic field is applied. This causes the fluid to stiffen locally, forming a "polishing ribbon" that conforms to the surface of the workpiece. The suspended abrasives in the stiffened ribbon remove material gently but effectively through micro-cutting and shear mechanisms.

A schematic overview of the MRP process is shown in Figure 1.3, illustrating the interaction between the magnetic field, fluid, and the rotating workpiece. The controlled nature of the polishing ribbon ensures that only minimal, precise amounts of material are removed, which is ideal for complex optical surfaces and components requiring high shape accuracy and low surface roughness.

The non-contact and programmable nature of the process also makes it suitable for delicate materials and free-form geometries. MRP is particularly advantageous for finishing brittle and hard materials like glass, ceramics, and certain metals, offering nanometre-level control over surface quality and form accuracy [15].

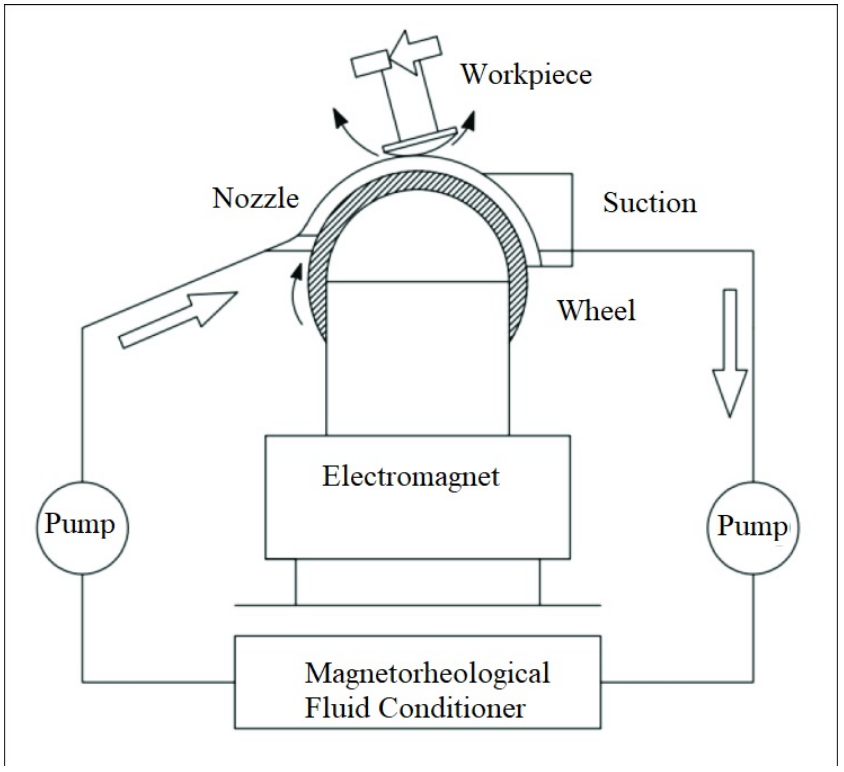

FIGURE 1.3: Schematic diagram of the MRP process. Source [16]

1.2.4 Ultrasonic Polishing

Ultrasonic Polishing is a precision surface finishing technique that combines mechanical abrasion with high-frequency ultrasonic vibrations to achieve fine material removal [17]. In this method, a tool, often shaped to match the geometry of the workpiece, is vibrated at ultrasonic frequencies, typically around 20–40 kHz, while abrasive slurry is delivered between the tool and the workpiece. The ultrasonic energy induces micro-cavitation and enhances the momentum of abrasive particles, enabling efficient and uniform polishing, particularly in intricate geometries and tight spaces. Compared to conventional mechanical methods, ultrasonic polishing significantly reduces thermal and mechanical stress, making it highly effective for brittle and delicate components. A schematic of the process is shown in Figure 1.4.

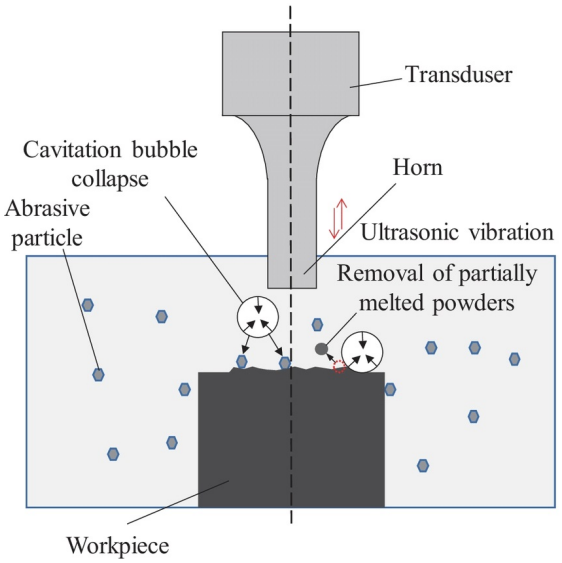

FIGURE 1.4: Schematic diagram of Ultrasonic Polishing. Source [18]

The localized energy delivered by ultrasonic vibrations disrupts the surface boundary layer, allowing the abrasive particles to access micro-scale asperities and remove them effectively. This non-directional process is particularly useful for polishing complex components like micro-molds, optical cavities, and high-aspect-ratio features. Materials such as hardened steels, ceramics, and carbides, known for their machinability challenges, can be polished to nanometric finishes without inducing subsurface cracks or distortion, demonstrating the versatility and precision of ultrasonic polishing.

1.2.5 Bonnet Polishing

Bonnet polishing is a precision surface finishing process that employs a flexible, rotating polishing tool, resembling a soft bonnet or spherical cap, along with an abrasive slurry to achieve controlled material removal [19]. The process was originally developed for the fabrication of large optical components, but it has since been adapted for a variety of high-precision applications, including free-form surfaces and complex geometries that are difficult to polish using traditional rigid tools [20].

At the heart of bonnet polishing is the compliant tool, typically a rubber or polyurethane bonnet mounted on a rotating spindle, which conforms to the surface

of the workpiece. This compliance enables the tool to maintain consistent contact pressure across curved or uneven surfaces. The bonnet is coated with a polishing pad and infused with an abrasive slurry, allowing the system to perform localized and gentle material removal. By carefully controlling process parameters such as pressure, tool tilt, dwell time, and rotational speed, bonnet polishing can achieve sub-micrometer surface finishes and nanometre-level roughness. A schematic of bonnet tool is given in the Fig. 1.5.

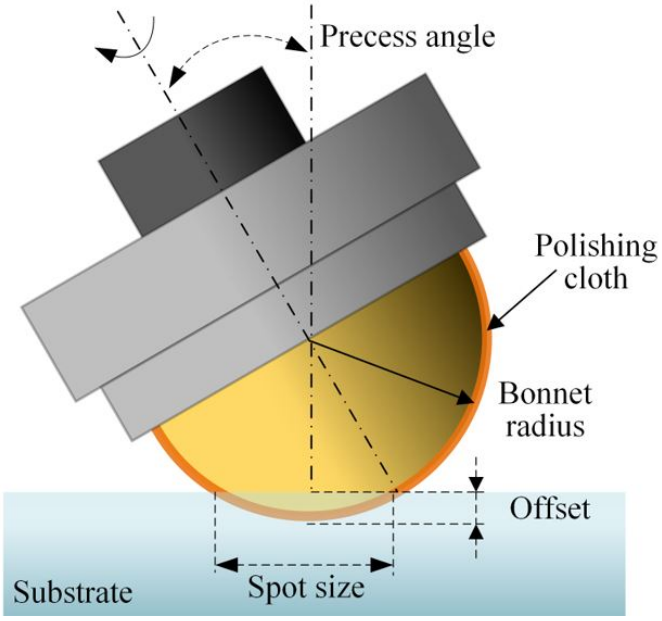

FIGURE 1.5: Schematic diagram of a typical bonnet tool, taken from [21]

Bonnet polishing offers several key advantages that make it well-suited for ultra-precision surface finishing. One of the primary benefits is the flexibility of the inflatable bonnet, which allows it to conform to the surface of the workpiece. This enables uniform material removal even on complex geometries, resulting in high surface finish accuracy. Additionally, the low-pressure and low-temperature nature of the process minimizes the risk of inducing micro-cracks or residual stresses, preserving the integrity of delicate materials. Bonnet polishing is also highly versatile, being compatible with a wide range of substrates such as glass, ceramics, metals, and optical polymers. Its adaptability extends across different component sizes—from miniature optical parts to large-scale optical systems. Furthermore, the polishing process is highly controllable via parameters such as pressure, dwell

time, and tool-path, making it ideal for integration into robotic or CNC-based polishing systems.

Despite these advantages, one of the most critical and challenging aspects of bonnet polishing is predicting the Material Removal Rate (MRR). Unlike rigid tools where removal rates can be more directly modelled, bonnet polishing involves complex interactions between tool deformation, slurry flow, surface geometry, and process parameters. Traditional models such as Preston's equation provide a starting point but often fall short when precise control is required, especially under varying conditions. This is where machine learning (ML) offers significant potential. By leveraging experimental data and process feedback, ML algorithms can model the non-linear behaviour of MRR in bonnet polishing with greater accuracy than empirical equations alone. Integrating such models into the polishing system can pave the way for closed-loop control, self-optimization, and intelligent automation, bringing bonnet polishing into the realm of Industry 4.0 and beyond.

1.3 Material Removal Rate (MRR)

Material Removal Rate (MRR) is a fundamental performance metric in any subtractive manufacturing or finishing process, representing the volume or depth of material removed per unit time. In polishing operations, especially those targeting high precision, MRR is not only a measure of efficiency but also a critical factor in surface accuracy, uniformity, and process control. In most polishing processes, the goal is not merely to remove material quickly but to do so predictably, uniformly, and controllably. Too high of an MRR can result in over-polishing, surface defects, or deviation from desired profiles. Too low of an MRR leads to increased process time and reduced throughput. Therefore, understanding and accurately predicting MRR is essential for process planning, quality assurance, and automation [22].

Traditionally, MRR in polishing has been described using Preston's Equation, which assumes a linear relationship between material removal and the product of contact pressure and relative velocity [23]:

$$\text{MRR} = k \cdot p \cdot v \tag{1.1}$$

Where:

- k is the Preston coefficient (dependent on material and slurry conditions),
- p is the contact pressure,
- v is the relative velocity between tool and workpiece.

While Preston's equation provides a useful approximation for predicting material removal, it falls short in capturing the complex non-linearities and multifactor interactions present in real-world bonnet polishing processes. Factors such as tool deformation due to bonnet compliance, local surface curvature, slurry distribution and viscosity, temperature variations, and variations in tool tilt angle and dwell time all contribute to the material removal rate in interdependent and dynamic ways. These interactions are difficult to model using purely analytical approaches. Consequently, empirical models based on Preston's framework often require extensive calibration and still struggle to maintain accuracy when process conditions vary.

This inherent complexity makes MRR an ideal candidate for data-driven modelling using machine learning techniques. ML can learn patterns and relationships from historical data, enabling it to predict MRR under diverse process conditions with higher accuracy. By training algorithms such as regression trees, support vector machines, or neural networks on experimental data, it becomes possible to develop predictive models that support real-time decision-making and process optimization.

In this thesis, MRR prediction serves as the core application of machine learning. Accurate MRR models are a stepping stone toward automating the bonnet polishing process, enabling dynamic adjustments based on surface feedback, and reducing reliance on trial-and-error calibration. Ultimately, this improves productivity, consistency, and surface quality across varying polishing tasks.

1.4 Background

As manufacturing demands continue to evolve toward greater complexity and tighter tolerances, there has been a marked shift toward automation and data-driven control across various industrial processes [24, 25]. Polishing, a critical step in surface finishing for precision components, has traditionally depended on operator expertise and manual adjustments. However, with increasing emphasis on consistency, traceability, and real-time responsiveness, industries are now embracing intelligent process control strategies to augment both accuracy and productivity. This transition is particularly evident in high-precision sectors like optics and aerospace, where even microscopic surface deviations can compromise functionality [26].

Bonnet polishing has emerged as a favoured technique for achieving ultra-smooth finishes on intricate and free-form surfaces due to its compliance, flexibility, and ability to uniformly conform to complex topographies [19]. Despite these strengths, the process remains difficult to model and control precisely, primarily due to the non-linear interactions among parameters such as tool pressure, dwell time, bonnet deformation, and slurry characteristics. Accurate prediction of the Material Removal Rate (MRR) is vital, yet conventional physics-based models like Preston's equation often fall short under such dynamic conditions. These models assume linear dependencies and steady-state interactions, failing to capture the rich variability present in real-world polishing environments.

To overcome these limitations, machine learning (ML) has been increasingly explored for its capacity to model non-linear systems directly from data without requiring analytical simplifications. While ML has found successful applications in other subtractive manufacturing processes, such as turning [27], grinding [28], and planar polishing [29], its potential in bonnet polishing remains underutilized. This thesis addresses this research gap by developing a data-driven framework for MRR prediction using force and slurry sensor data collected during the polishing process.

By integrating domain-specific feature engineering with advanced ML models, including a hybrid architecture that combines a Multi-Branch Attention Residual CNN (MARCNN) and an Artificial Neural Network (ANN)—the study demonstrates a pathway toward intelligent, adaptive control of polishing operations. This aligns with the broader objectives of Industry 4.0, contributing to the vision of smart, self-optimizing manufacturing systems.

1.5 Problem Description

While polishing is a widely researched surface finishing process, the specific technique of bonnet polishing remains relatively under explored, particularly from the perspective of intelligent automation and advanced machine learning integration. Figure 1.6 illustrates the conventional workflow adopted in previous studies for predicting MRR during bonnet polishing. As evident, the process involved manual data trimming, basic feature extraction, and a simple predictive model, which not only limit scalability but also delay the feedback loop. These limitations form the core motivation for this research.

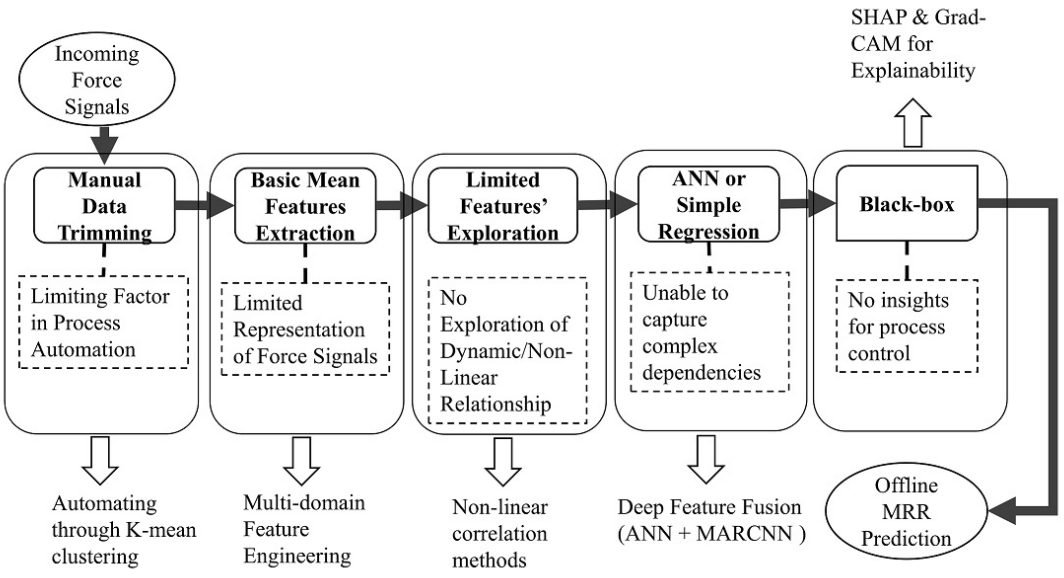

FIGURE 1.6: Conventional bonnet polishing pipeline and associated limitations that this study aims to resolve.

Existing literature predominantly focuses on conventional polishing processes or adopts traditional modelling techniques such as Artificial Neural Networks (ANN), Random Forest (RF), and Extreme Gradient Boosting (XGBoost) for predictive tasks like Material Removal Rate (MRR) estimation. However, these approaches often fall short in capturing the complex, non-linear, and high-dimensional nature of real-world bonnet polishing dynamics.

Furthermore, many of the existing studies do not utilize state-of-the-art deep learning architectures that are better suited for learning from multi-modal time series data. Architectures such as Convolutional Neural Networks (CNNs), particularly those enhanced with attention mechanisms, residual connections, and multi-branch pathways, have shown significant potential in other domains but remain largely untapped in the context of bonnet polishing.

Another major limitation observed in current research is the lack of full automation in the data preprocessing pipeline. For instance, force data acquired from six-axis load cell sensors installed beneath the worktable are often manually processed to remove irrelevant segments, such as pre-cut and post-cut regions, and manually aligned for analysis. This introduces human bias, increases labour, and hinders scalability and reproducibility.

Moreover, the structure of the data itself is often underutilized. The force data comprising one sensor along the X-axis, two along the Y-axis, and three along the Z-axis, are rich in both temporal and spectral information. However, previous studies typically neglect multi-domain feature extraction methods such as frequency domain transforms or discrete wavelet transform (DWT), thereby failing to leverage richer signal representations. An equally important omission is the exclusion of critical process parameters such as slurry conditions, particularly pH and temperature, which significantly influence the material removal characteristics but are not integrated into most predictive models to date.

Given these limitations, there is a clear need for a comprehensive, automated, and intelligent framework that:

- Utilizes advanced deep learning architectures, such as a multi-branched CNN with attention and residual connections (MARCNN).
- Integrates domain fusion by combining time-domain, frequency-domain, and DWT-based signal representations.
- Incorporates slurry parameters (pH and temperature) into the predictive model.
- Automates preprocessing steps like force data alignment and irrelevant region removal.
- Explores deep feature fusion strategies combining MARCNN with existing methods such as ANN.

This research aims to address these gaps by developing a robust machine learning pipeline for accurately predicting MRR in bonnet polishing, thereby advancing the field toward smarter and more autonomous precision manufacturing.

1.6 Motivation

In high-precision manufacturing, surface quality is a critical factor that directly influences the performance, durability, and optical clarity of components, particularly in industries such as aerospace, optics, and semiconductors. Bonnet polishing, known for its ability to deliver ultra-smooth surfaces with minimal subsurface damage, plays a vital role in such applications. However, despite its importance, the process remains largely semi-automated and heavily reliant on manual intervention for tasks such as data alignment and preprocessing. This limits its scalability and consistency, especially in industrial settings where precision and throughput are paramount.

Moreover, the prediction of Material Removal Rate (MRR) requires robust modelling of complex, non-linear relationships involving multiple process variables.

Traditional machine learning approaches such as ANN, Random Forest, and XGBoost often lack the architectural depth and feature abstraction capabilities necessary to capture the intricate dynamics of bonnet polishing. These models also tend to overlook valuable signal characteristics and process parameters, such as multi-domain features (time, frequency, wavelet) and slurry properties (pH, temperature), which significantly influence the polishing outcome.

With the rapid advancement of deep learning and signal processing techniques, there exists a strong opportunity to reimagine the bonnet polishing workflow through automation and intelligent prediction. Architectures such as multi-branched convolutional neural networks (CNNs) augmented with attention mechanisms and residual connections offer a powerful means to extract hierarchical features from multi-dimensional sensor data. Coupled with deep feature fusion method and the integration of richer, multi-domain features, these methods promise substantial improvements in both predictive accuracy and operational efficiency. The motivation for this research arises from the need to bridge this technological gap by designing a fully automated, data-driven framework capable of predicting MRR with high fidelity. By addressing the limitations of current approaches and integrating modern machine learning techniques, this study aims to contribute toward the evolution of intelligent polishing systems that are not only more accurate, but also more autonomous, scalable, and industrially viable.

1.7 Scope of the Study

This research is focused on augmenting the bonnet polishing process through a data-driven framework that enables near real-time prediction of MRR using force sensor and slurry parameter data. In existing literature, the process involved manual data trimming, basic feature extraction, and a simple predictive model, which not only limit scalability but also delay the feedback loop.

These limitations form the core motivation for this research. In contrast, the present study aims to automate and augment the polishing pipeline by integrating

advanced clustering, multi-domain features, deep feature fusion, and explainable AI techniques. These limitations, along with the corresponding solutions and adopted methodologies, are systematically illustrated in the conceptual block diagram presented in Fig. 1.7.

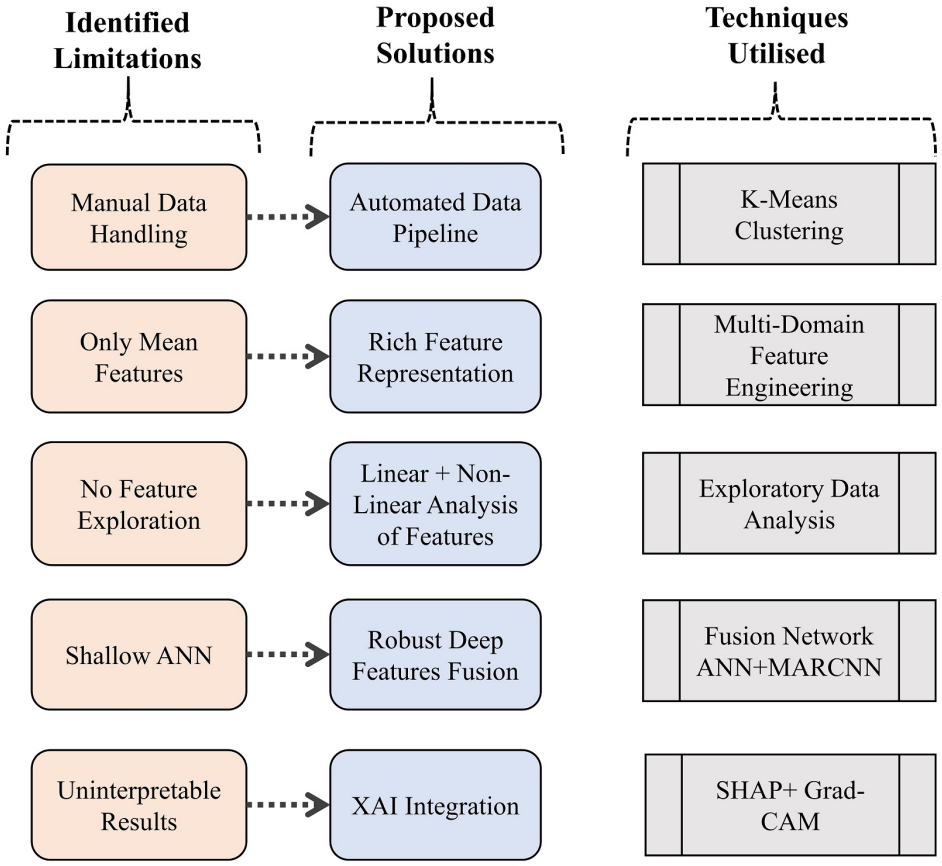

FIGURE 1.7: Block diagram highlighting identified limitations, achieved improvements, and adopted techniques.

The scope of this study encompasses the following key components:

1.7.1 Automating Signal Segmentation

Polishing force signals acquired from experiments often contain non-productive segments due to manual triggering, including pre- and post-polishing intervals. To eliminate the need for manual trimming, which is an error-prone and time-intensive task, this study introduces an automated segmentation mechanism using K-means clustering.

This unsupervised technique effectively isolates the valid polishing region from raw force data, forming a critical first step in enabling scalable data preprocessing.

1.7.2 Enhancing Feature Representation

Capturing the complex physical behaviour of the polishing process forces requires richer signal descriptions than conventional single-domain features. This challenge is addressed through multi-domain feature engineering of the force signals that extracts informative characteristics from the time domain (e.g., RMS, skewness), frequency domain (e.g., spectral energy, entropy), and wavelet domain (e.g., approximation coefficients from DWT).

This integrated feature design strengthens the model's ability to generalize across variable polishing conditions.

1.7.3 Refining Inputs via Feature Selection

To minimize redundancy and improve the focus of the model on meaningful patterns, a comprehensive exploratory data analysis (EDA) is performed using Pearson and distance correlation techniques.

This facilitates the elimination of low-impact features, effectively reducing model complexity without compromising predictive accuracy.

1.7.4 Improving Model Accuracy through Deep Learning

The inherently non-linear and multi-factor nature of bonnet polishing limits the applicability of shallow models. To capture these deeper insights, a Multi-Branched Attention Residual Convolutional Neural Network (MARCNN) is employed. Its architecture allows the model to learn hierarchical patterns and interactions across the extracted domains, boosting predictive capability beyond traditional ANN baselines.

1.7.5 Ensuring Robustness via Deep Feature Fusion Technique

Predictive reliability is further enhanced by combining the MARCNN with an Artificial Neural Network (ANN) through an deep feature fusion approach. This strategy leverages complementary strengths of both models, where the ANN handles statistical mean features and the MARCNN processes domain featues, to deliver robust MRR predictions under changing operational scenarios.

1.7.6 Improving Model Insight

A common drawback of deep learning systems is their "black-box" nature. To address this, explainable AI techniques are embedded within the framework. SHAP (SHapley Additive exPlanations) is applied to the ANN branch to quantify feature contributions, while Grad-CAM (Gradient-weighted Class Activation Mapping) visualizes influential regions in the CNN filters of the MARCNN branch. These tools offer insights into model behaviour, making results more transparent and actionable for process engineers. The study is conducted entirely using pre-existing sensor data and infrastructure. No hardware alterations, new sensor additions, or physical redesigns of the polishing setup are undertaken. The focus is exclusively on automating and advancing the computational aspects of polishing process monitoring and control.

1.8 Objectives

The primary objective of this thesis is to automate the data pipeline and enhance the prediction accuracy of the bonnet polishing process through advanced machine learning techniques. The step-wise methodological pipeline adopted in this study, aligned with the key objectives and corresponding contributions, is illustrated in Fig. 1.8. It presents the progression from automated preprocessing to explainable

prediction, highlighting each stage's specific contribution toward improving the bonnet polishing process.

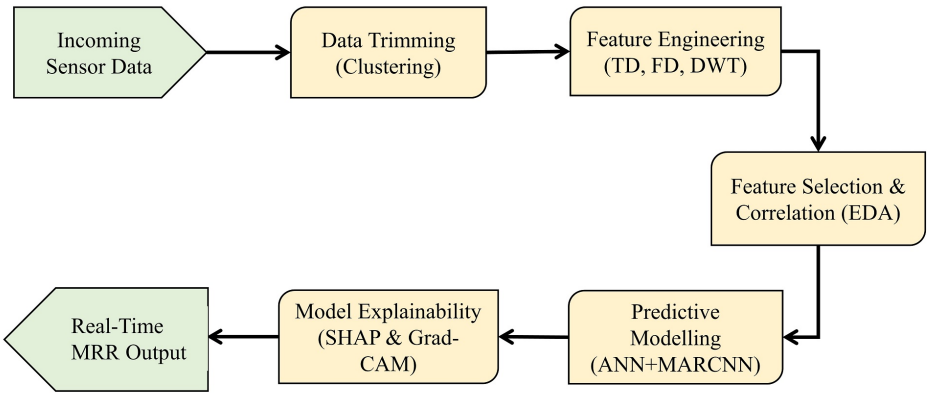

FIGURE 1.8: Block diagram illustrating the step-wise methodological contributions adopted in this study.

The specific objectives of the study are as follows:

1. To implement an automated data preprocessing pipeline that eliminates manual intervention, particularly by segmenting the effective polishing region using K-means clustering.

2. To extract meaningful features from multi-sensor force data in the time domain, frequency domain, and wavelet domain (DWT), and to incorporate slurry parameters such as pH and temperature into the feature set.

3. To perform exploratory data analysis (EDA) for selecting the relevant features using both the linear and non-linear correlation analysis.

4. To enhance the predictive performance for MRR prediction by developing a deep learning-based predictive model using a Multi-branched Attention Residual Convolutional Neural Network (MARCNN) architecture.

5. To improve overall prediction accuracy and robustness by fusing the deep features from the proposed model with baseline model such as ANN.

6. To enhance the transparency and practical interpretability of the model for process engineers by integrating explainable AI techniques across both the ANN and MARCNN branches.

1.9 Thesis Overview

This thesis is organized into eight chapters, each systematically contributing to the development of a data-driven and automated framework for predicting the Material Removal Rate (MRR) in the bonnet polishing process. The overview of each chapter is as follows:

- **Chapter 1 – Introduction, Problem Framing, and Research Objectives**

  This chapter introduces the importance of surface finishing in high-precision manufacturing, with a focus on bonnet polishing. It outlines the motivation for automating the polishing process, defines the problem statement, states the research objectives, and presents the scope and contributions of the work.

- **Chapter 2 – Survey of Prior Work and Identified Gaps**

  A critical review of existing literature on MRR modelling through basic and extended empirical approaches is given in this chapter. It mainly reviews the contemporary approaches in data-driven MRR modelling in bonnet polishing. It also highlights limitations in current methods and identifies key research gaps that motivate the proposed work.

- **Chapter 3 – Experimental Setup and Dataset Description**

  This chapter details the physical setup used for experimentation. It also describes the structure and characteristics of the dataset generated from the experimental runs.

- **Chapter 4 – Data Acquisition and Preprocessing**

  Discusses the acquisition of raw sensor data and outlines the steps taken

to clean and prepare it for analysis. An automated data pipeline, based on unsupervised learning, is developed for the identification and removal of non-representative data signals. It also details the alignment and tilt correction of the MRR data.

- **Chapter 5 – Multi-Domain Feature Engineering and Data Exploration**

  Presents the strategies used to extract informative features from time-domain, frequency-domain, and wavelet-domain representations of the force signals. Additionally, it includes exploratory data analysis using correlation techniques to assess feature relevance and redundancy.

- **Chapter 6 – Machine Learning Model Development for MRR Prediction**

  Describes the model architectures used in this study, including an Artificial Neural Network (ANN), a Multi-Branch Attention Residual Convolutional Neural Network (MARCNN), and a deep feature fusion combining both. It also introduces the evaluation metrics used to assess model performance.

- **Chapter 7 – Results and Discussions**

  Presents and analyses the results of model training and validation. Comparative performance between models, ablation studies on architectural components, and discussions on the impact of automation and feature strategies are thoroughly addressed. Explainability techniques such as SHAP and Grad-CAM are also discussed.

- **Chapter 8 – Conclusion and Future Work**

  Summarizes the key findings and contributions of the research. It also discusses the directions for future research, including real-time deployment, model generalization, and broader integration into smart manufacturing systems.

Chapter 2

Survey of Prior Work and Identified Gaps

Material Removal Rate (MRR) prediction has long been central to the advancement of polishing technologies, as it directly affects surface quality, dimensional accuracy, and process efficiency. In high-precision applications such as optics manufacturing, aerospace finishing, and semiconductor fabrication, the ability to precisely control MRR is vital for achieving tight tolerances and minimizing surface or subsurface damage [30, 31]. While a variety of techniques have been developed to model and predict MRR, polishing processes, especially those involving free-form or complex geometries, remain difficult to model due to their inherently non-linear and time-varying dynamics.

Among various polishing methods, bonnet polishing stands out as a particularly adaptable and effective technique for complex surface finishing. It utilizes an inflatable, compliant tool (the bonnet), which conforms to the local surface topography of the workpiece, allowing for better control of pressure distribution and surface conformity. Despite these advantages, accurately predicting MRR in bonnet polishing remains challenging due to the intricate interaction between the tool, slurry, and workpiece. Variability in contact conditions, material responses, and process parameters introduces significant non-linearities and transient behaviours that limit the effectiveness of conventional models [32, 33].

2.1 Traditional MRR Estimation

Historically, MRR modelling has been rooted in analytical approaches. One of the earliest and most widely adopted formulations is Preston's equation [23], which postulates a linear relationship between MRR, pressure, and relative velocity. While Preston's model has laid the foundation for understanding polishing dynamics, its simplifying assumptions restrict its applicability, especially in advanced or non-uniform polishing environments.

Recognizing these limitations, researchers have extended Preston's equation to include dwell time, contact area, tool wear, and slurry behaviour [34–37]. These extensions improved alignment with experimental results but still fell short in handling dynamic process variability, particularly in bonnet polishing where real-time changes are common [38–40].

2.2 Data-Driven MRR Estimation

To overcome these inherent limitations, the research community has increasingly turned to data-driven modelling techniques. Machine learning (ML) methods offer a fundamentally different approach: instead of relying on fixed equations, ML models learn patterns from historical data, capturing complex and non-linear relationships among process parameters and MRR outcomes. This adaptability makes ML particularly suitable for polishing applications characterized by dynamic tool-material interactions and sensor-based variability [33, 41].

Applications of ML in polishing have expanded across various domains, including chemical mechanical polishing (CMP), magneto-rheological finishing, and robotic polishing. In these contexts, features such as polishing force, relative motion, process time, and even environmental parameters like temperature and slurry pH have been employed to train predictive models [42–44].

ML models not only offer improved prediction performance but also serve as a stepping stone toward automation and real-time closed-loop control.

2.2.1 Correlation of Polishing Forces and MRR

A significant body of literature supports the strong correlation between polishing forces and MRR across various polishing modalities. A study [45] proposed a deterministic model for MRR in bonnet polishing based on online-acquired frictional and normal forces, experimentally validating their predictive relevance. Similarly, another study [46] developed a robotic polishing system where controlling polishing forces was critical to achieving a uniform removal rate. In magnetorheological polishing, this study [47] showed that penetration depth, and thus removal rate, depends strongly on drag and normal forces, achieving a model R^2 of 0.99 for glass polishing.

In the domain of Chemical Mechanical Polishing (CMP), a clear linear relationship between frictional and normal forces and MRR was shown in [48] using 2D force measurements. More recent studies integrating machine learning have continued to emphasize the role of force data. Jeong et al.[49] showed polishing pressure, which is polishing force applied per unit area, to be a highly correlated feature for MRR prediction in CMP using a deep feature fusion. Likewise, Li et al.[50] identified downward polishing pressure as one of the top predictive features using decision-tree-based ensemble learning. In robotic polishing contexts, Schneckenburger et al.[51] demonstrated that the normal force (Z-axis), in combination with speed and time, served as effective input features for predicting MRR in glass polishing.

These studies underscore the critical role of force-related features in predictive modelling of MRR and provide a strong foundation for exploring machine learning-based approaches, which have gained increasing traction in recent years for capturing the non-linear and dynamic nature of polishing processes.

2.2.2 Deep Learning Techniques for MRR

Among the broad range of ML models, deep learning techniques, particularly deep neural networks (DNNs), have shown exceptional capability in extracting multi-level representations from raw sensor and process data [52–54]. Convolutional

Neural Networks (CNNs), in particular, are well-suited to processing structured data like time series and signals due to their locality-preserving operations. More advanced architectures such as Residual CNNs (ResCNNs), which incorporate shortcut connections to mitigate vanishing gradients, have shown superior performance in MRR prediction tasks [41]. Additionally, biologically inspired models like Deep Belief Networks (DBNs) and evolutionary-optimized architectures have been explored for their ability to generalize from complex datasets [55].

Nevertheless, deep learning models come with challenges, among them is the requirement for large datasets, which are often difficult to obtain in experimental or limited-run industrial settings. In response, researchers have investigated two major strategies: data augmentation or fusion, and model architectural improvements. Of these, the latter offers a more practical path in scenarios where data collection is costly or time-consuming. Recent trends emphasize the importance of robust architectures that perform well under limited-data regimes, such as lightweight CNNs, attention mechanisms for feature re-weighting, and deep feature fusion approaches.

Deep feature fusion techniques have gained particular traction in this context. By combining the outputs of multiple base learners, either of the same or different types, deep feature fusion methods reduce model variance and improve generalizability [56, 57]. In polishing research, ensembles have been constructed using LSTM, ANN, and tree-based models, with improved prediction accuracy reported through feature-level fusion and multi-stage regression pipelines [58]. These architectures benefit from diversity in both input features and model structure, often leading to more robust predictions.

2.2.3 Multi-Domain Features

A key enabler of better performance gains for predictive analytics is the use of rich, multi-domain input features. Time-domain (TD), frequency-domain (FD), and time-frequency domain features such as those from Discrete Wavelet Transform (DWT) each contribute unique insights. TD features capture statistical

properties of the signal, FD features expose harmonic content, while DWT isolates localized transient behaviour. When fused, these domains enable the model to build a more comprehensive understanding of the underlying polishing dynamics [59, 60]. A study [61] adopted statistical time-domain features for defect classification in polishing and reported improved accuracy when combined with Gabor filter features, achieving up to 82% classification accuracy. Another study [62], specifically on bonnet polishing proposed a frequency-domain characterization approach to address surface ripple formation. By linking spatial process parameters with frequency-domain evaluation indices, the work demonstrated how tool geometry and contact conditions influence ripple mitigation.

In roboticized polishing of aero-engine blades [63], vibration signals were analysed to diagnose contact faults. Eleven time-domain features were extracted from the signals, and a whale optimization algorithm SVM model was used for classification, achieving effective real-time fault detection. In laser polishing, acoustic emission signals have been analyzed in the time–frequency domain to enable online monitoring and process state classification [64]. Wavelet-based noise reduction and feature extraction were applied, and a BP neural network model achieved a classification accuracy of 97.7%.

Another study [65] on robot-assisted polishing extracted features from force signals in both the time and frequency domains to estimate surface roughness. The results showed that combining TD and FD features provided valuable information for identifying the polishing end point. In roboticized polishing of aero-engine blades, vibration signals were analysed to diagnose contact faults [64]. Eleven time-domain features were extracted from the signals, and a whale optimization algorithm–SVM model was used for classification, achieving effective real-time fault detection.

Overall, while polishing research has increasingly adopted domain features from time, frequency, and time-frequency for tasks such as defect classification, fault diagnosis, and process monitoring, their systematic integration in bonnet polishing remains scarce, highlighting a clear gap and the need for comprehensive multi-domain feature approaches.

2.3 Limitations in the Existing Literature

Despite substantial progress in modelling and predicting MRR using both analytical and ML techniques, several critical gaps remain, particularly in the context of automation, real-time integration, and smart process monitoring in bonnet polishing. Firstly, a major limitation lies in the manual nature of data preprocessing. Most existing studies rely on human intervention to isolate valid polishing segments within force signal data, such as trimming pre- and post-polishing regions. This method is time-consuming, error-prone, and inconsistent, especially when dealing with large datasets or real-time applications. The absence of automated segmentation techniques, such as unsupervised clustering, significantly limits the scalability and industrial applicability of current solutions.

Another gap involves the either basic, such as mean features, or fragmented approach to feature engineering. Several studies have focused on individual feature domains, such as time-domain, frequency-domain, but have not unified them into a cohesive, multi-domain framework. This results in incomplete process representation, thereby reducing the generalizability and accuracy of predictive models under varying polishing conditions. There is a clear need for comprehensive feature fusion strategies that capture the multifaceted nature of the polishing process.

Moreover the advanced and hybrid model architectures are underutilized. Most existing research focuses on single-branch neural networks or traditional ML algorithms that do not leverage the strengths of deep feature fusion or modular designs. The use of hybrid systems, such as those combining ANN with multi-branch CNNs incorporating attention and residual mechanisms, remains largely unexplored. Such architectures are essential for learning from diverse and complex input features while maintaining robustness across various polishing scenarios. Lastly, the explainability of ML models, which are considered as "black boxes", is rarely addressed. With increasing model complexity, particularly in deep learning approaches, there is a growing demand for interpretable outputs that can provide actionable insights to process engineers. However, explainable AI (XAI) tools such as SHAP (SHapley Additive exPlanations) and Grad-CAM (Gradient-weighted

Class Activation Mapping) are rarely employed in polishing studies. Without these, the models remain black boxes, limiting trust and practical deployment by process engineers in production environments.

Addressing these gaps is crucial for developing intelligent, self-correcting polishing systems capable of operating in dynamic manufacturing environments. This thesis aims to bridge these shortcomings by proposing a fully automated, explainable, and multi-domain deep feature fusion framework for MRR prediction, advancing towards smarter polishing solutions which are aligned with Industry 4.0 objectives.

Chapter 3

Experimental Setup and Dataset Description

This study builds upon the experimental foundation established in previous work [33] and [66], extending the methodology by incorporating deep feature fusion models for enhanced material removal rate (MRR) prediction. The experimental setup was designed to capture high-resolution polishing force data alongside slurry process parameters during bonnet polishing of fused silica optics. An overview of the entire experimental and modelling pipeline is depicted in Fig. 3.1, which presents a schematic flowchart illustrating the sequence of processes from data acquisition to final material removal prediction.

3.1 Machine Setup

Experiments were conducted using a 7-axis CNC Zeeko Intelligent Robotic Polisher (IRP600) located at the University of Huddersfield's Laboratory for Ultra Precision Surfaces. The system was configured with an inflatable R40 bonnet tool covered in polyurethane cloth, and a slurry recirculation system using cerium oxide-based Super Cerox 1663. The tool followed a raster-style scanning pattern during polishing as given in the Fig. 3.2, designed to ensure even material removal across the polishing field.

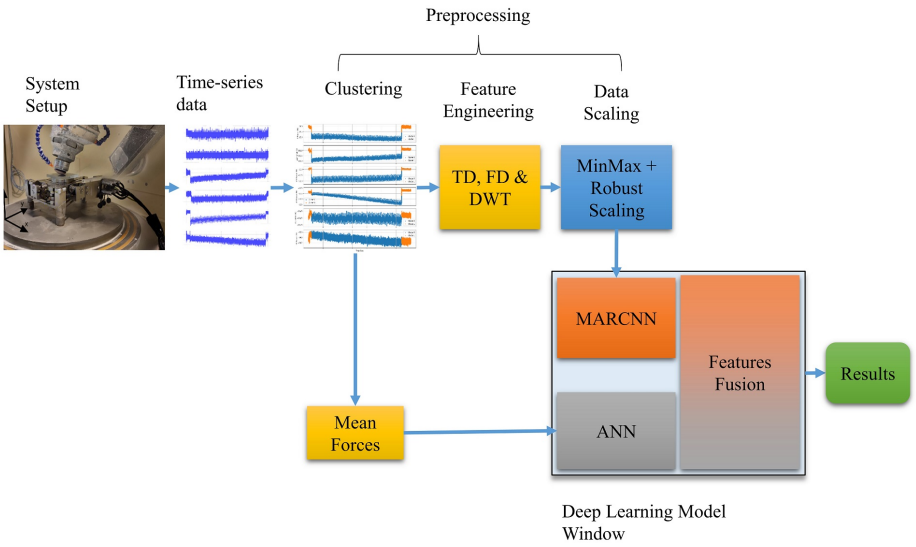

FIGURE 3.1: Overview of the experimental and modelling pipeline. The process begins with multi-source signal acquisition and proceeds through clustering, feature engineering, and prediction via the deep feature fusion using ANN-MARCNN model.

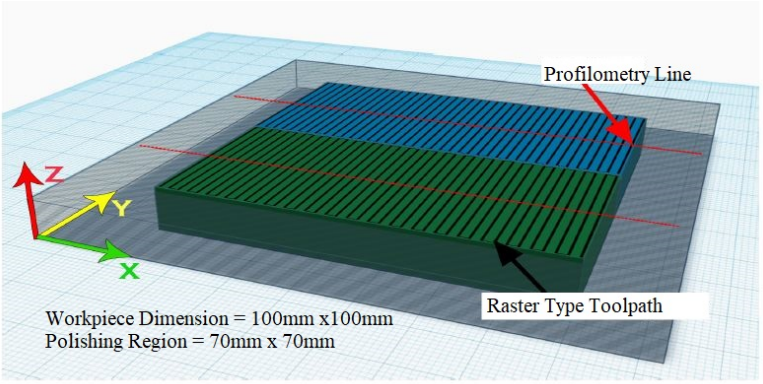

FIGURE 3.2: Raster tool path used during bonnet polishing. Profilometry lines show the line across which measurements in Z-axis were taken [66]

The square fused silica workpieces, each measuring 100 mm × 100 mm, were polished within a central 70 mm × 70 mm region. This centre zone was intentionally isolated from the outer 15 mm border to prevent edge-related force anomalies and to facilitate repeatable metrology. The central field was further divided into two subregions, Y- and Y+, allowing consecutive runs without repositioning the part between trials. The tool-path raster pattern was aligned along the X-axis for consistency in both processing and subsequent surface metrology.

3.1.1 Instrumentation and Sensor Integration

The polishing assembly was mounted on a custom-designed force table fixed atop the machine's rotary axis. As shown in Fig. 3.3, six piezo-resistive load cell sensors were distributed along the three axes: one in X, two in Y, and three in Z. This arrangement enabled real-time capture of multi-directional polishing forces.

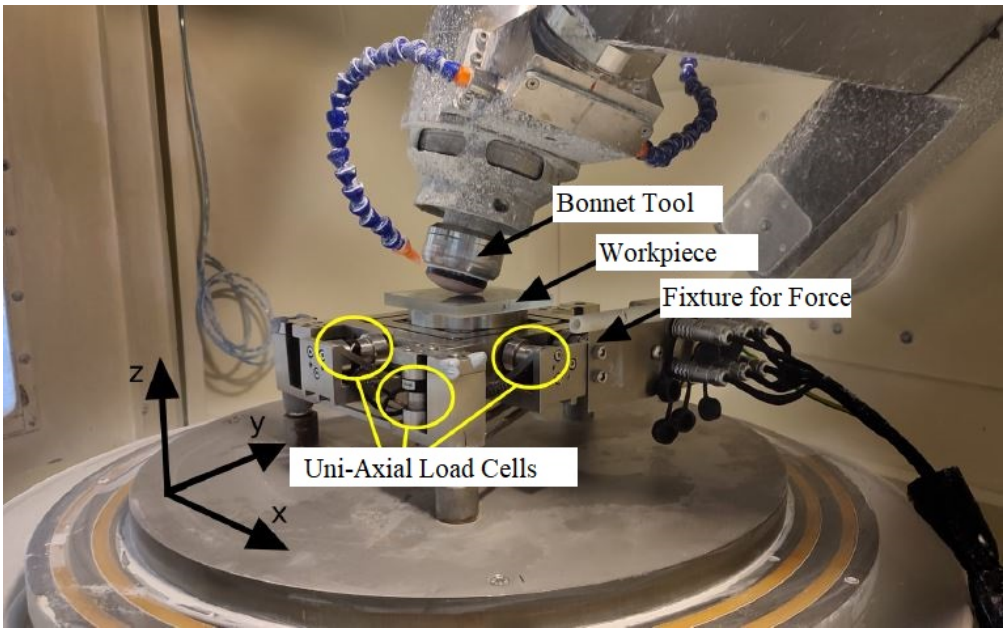

FIGURE 3.3: Experimental setup showing the mounted workpiece, inflatable bonnet tool, custom force table, and connected data acquisition modules. [33]

Sensor signals were routed through the instruNet data acquisition system, comprising an iNet-400 card cage, iNet-410/420/430 DAQ cards, and an iNet-240 USB controller. Force data was sampled at 500 Hz to capture transient interactions between the tool and the workpiece. Simultaneously, slurry pH and temperature were monitored at 4 Hz using a Flat Surface PHE-6510B electrode and thermocouple sensor, respectively, both connected via iNet-510 and iNet-511 modules.

In addition to live sensor inputs, slurry property measurements were collected during polishing runs. Density and flow rate were recorded once per day before trials, while particle size distribution (PSD) was measured every 4 minutes using a Microtrack Nanotrac Flex analyser. Each PSD entry represented an average of three ten-second sub-scans to reduce measurement noise. Slurry samples were pipetted manually and transported for metrology in near real-time.

3.1.2 Surface Profiling and MRR Estimation

Surface profiles were recorded using a Taylor Hobson Form Talysurf Series 2 profilometer, offering vertical resolution down to 0.8 nm. Profilometry was performed before and after each polishing run along the X-axis across the middle of the polishing zone. Each scan extended 98 mm with a 1 mm buffer at both ends to prevent stylus overrun. A narrow trench was etched into the surface before the first polishing cycle to serve as a fixed reference point for profile alignment. The change in Z-values between pre- and post-polish scans was used to calculate material removal, which in turn allowed for MRR estimation per run.

3.1.3 Complete Experimental Protocol

The experimental campaign was carefully designed to capture comprehensive sensor-based information under controlled yet diverse polishing conditions. A total of 34 polishing runs were conducted on a fused silica workpiece using a fixed tool path and setup, while varying polishing time (5, 10, and 20 minutes) and surface feed rates (250, 500, and 1000 mm/min). This ensured the dataset included sufficient variation in force dynamics and material removal responses for robust modelling and generalizability. The process begins with raw signal acquisition from six piezo-resistive force sensors and additional slurry parameters (pH and temperature), recorded at 500 Hz and 4 Hz respectively. This raw data undergoes timeline-based segmentation and K-means clustering to remove non-polishing segments and isolate meaningful polishing-phase data. Feature extraction is then performed using two complementary schemes: time-averaged scalar features for the ANN branch, and time-frequency domain features for the MARCNN branch.

The predictive model architecture is divided into two distinct branches: the ANN branch processes mean features (forces, pH, and temperature), while the MARCNN branch employs multi-channel convolutional blocks enhanced with attention and residual mechanisms to capture localized and scale-invariant signal characteristics. The outputs of both branches are fused in a dense layer to yield the final

regression output: the predicted MRR. This structured pipeline demonstrates a data-centric approach, combining physical sensor signals with engineered features and deep learning, aiming to create a generalizable and interpretable model. The incorporation of domain-informed preprocessing, multi-domain feature engineering, and deep feature fusion underscores the novelty and engineering rigour of this approach.

3.2 Dataset Description

The dataset used in this work was obtained from 34 precision polishing runs performed on fused silica workpieces. Each run involved real-time acquisition of multiple signals, capturing both the mechanical response during polishing and associated slurry process parameters. The primary data sources include force signals measured via piezo-resistive load cells and environmental data such as slurry pH and temperature, acquired using dedicated sensors. These were sampled at 500 Hz and 4 Hz, respectively, using a LabVIEW-based data acquisition system connected through an instruNet i400 card cage and i240 USB interface.

3.2.1 Force Sensor Data

Six load cells were strategically positioned to capture polishing forces along all axes of motion: one sensor along the X-axis, two along the Y-axis, and three along the Z-axis. These sensors were mounted beneath the workpiece on a custom force table integrated into the IRP600 robotic system. The high-frequency sampling rate (500 Hz) was selected to capture the fine dynamic variations in contact forces, which are critical for accurate modelling of the material removal process. The raw force signals collected during each polishing run contain three distinct phases: pre-polishing, active polishing, and post-polishing. To ensure relevance, only data corresponding to the active polishing phase was retained using a clustering-based preprocessing approach described earlier.

3.2.2 Slurry Process Parameters

In addition to force measurements, two critical slurry process parameters, pH and temperature, were recorded in real time. These signals were captured using a Flat Surface PHE-6510B pH electrode and a thermocouple, respectively. Both sensors were immersed in a circulating slurry reservoir to ensure consistent readings and prevent sedimentation. The data acquisition for these sensors was conducted at 4 Hz, reflecting the relatively slow-changing nature of chemical and thermal parameters during polishing. While other slurry properties such as flow rate, density, and particle size distribution (PSD) were monitored manually during the experimental campaign, they were not included in this modelling work due to either low temporal resolution or manual sampling constraints. For instance, PSD data was collected manually every four minutes using the Microtrack Nanotrac Flex system, which limited its direct integration into real-time predictive modelling.

3.2.3 MRR Computation

The target variable, material removal rate (MRR), was not directly measured in real time. Instead, it was computed post-process by taking the difference in surface depth before and after polishing, as measured using a Taylor Hobson Form Talysurf Series 2 profilometer. The instrument offers a vertical resolution of 0.8 nm, ensuring accurate assessment of surface material removal. Measurements were taken along a predefined 98 mm track in the middle of the polishing zone, perpendicular to the raster tool path, with a 1 mm safety margin at the edges to avoid stylus damage. The central polishing zone was divided into two sub-regions (Y- and Y+) to enable sequential runs on the same workpiece.

3.2.4 Final Dataset Composition

Following signal cleaning and segmentation, the dataset was structured into two distinct feature sets customized to the deep feature fusion's architecture. The

methods adopted for structuring these datasets are described in the upcoming chapters:

3.2.4.1 ANN Input

Time-averaged scalar features, including mean values of forces from each axis (X, Y1, Y2, Z1, Z2, Z3).

3.2.4.2 MARCNN Input

Time-series representations of the polishing forces were segmented into 141 equal-length steps. For each segment, the following were extracted from all six force channels , along with average pH and temperature values for each polishing run.

- *Time-domain (TD)* features: Mean, standard deviation, RMS, skewness, kurtosis
- *Frequency-domain (FD)* features: Spectral energy and entropy using Power Spectral Density (PSD)
- *Wavelet-domain (DWT)* features: Mean of approximation coefficients using Daubechies-4 wavelet

This chapter presented a detailed overview of the experimental setup and the dataset used for MRR prediction in bonnet polishing. The dataset construction process included not only the capture of real-time multiaxial force signals and slurry parameters but also the computation of ground truth MRR using high-precision profilometry. The final dataset was structured to support a deep feature fusion architecture, with time-averaged scalar inputs fed into an ANN branch and segmented multi-domain features prepared for MARCNN processing. Altogether, the experimental setup and resulting dataset form a comprehensive and high-fidelity foundation for developing further techniques which are crucial for automating the data pipeline and extracting meaningful features from this data, which are explored in the subsequent chapters.

Chapter 4

Data Acquisition and Preprocessing

This chapter outlines the methodology developed for constructing an automated data pipeline aimed at predicting Material Removal Rate (MRR) in bonnet polishing processes. The approach integrates structured data preprocessing with data-driven modelling to overcome the limitations of traditional, manually intensive techniques. The chapter begins with a description of the data acquisition process, in which time series force signals and slurry parameters are collected from multiple polishing runs using force sensors and slurry monitoring instruments.

Given the manual nature of the data acquisition system, the recorded signals often include non-representative segments, specifically, pre- and post-polishing force data, which do not contribute to actual material removal. These irrelevant segments were previously removed through manual inspection, a process susceptible to inconsistency and human error. To address this, a clustering-based automation strategy is introduced to segment and exclude non-polishing intervals, thereby improving the reliability and repeatability of the dataset. Additionally, the MRR surface profile is preprocessed to correct for tilt and misalignment, utilizing a centrally engraved etching feature as a geometric reference. These preprocessing steps, profile correction, signal segmentation, and non-representative data elimination, lay the groundwork for robust model development. By automating input data

pipeline, the proposed pipeline enhances data quality and consistency, ensuring a reliable foundation for subsequent feature engineering and predictive modelling.

Figure 4.1 provides an overview of the automated preprocessing pipeline developed in this research. This pipeline spans two chapters: the current chapter focuses on data acquisition, signal alignment, and clustering-based segmentation, while Chapter 5 covers domain-specific feature extraction (Time-Domain, Frequency-Domain, and DWT) along with exploratory data analysis.

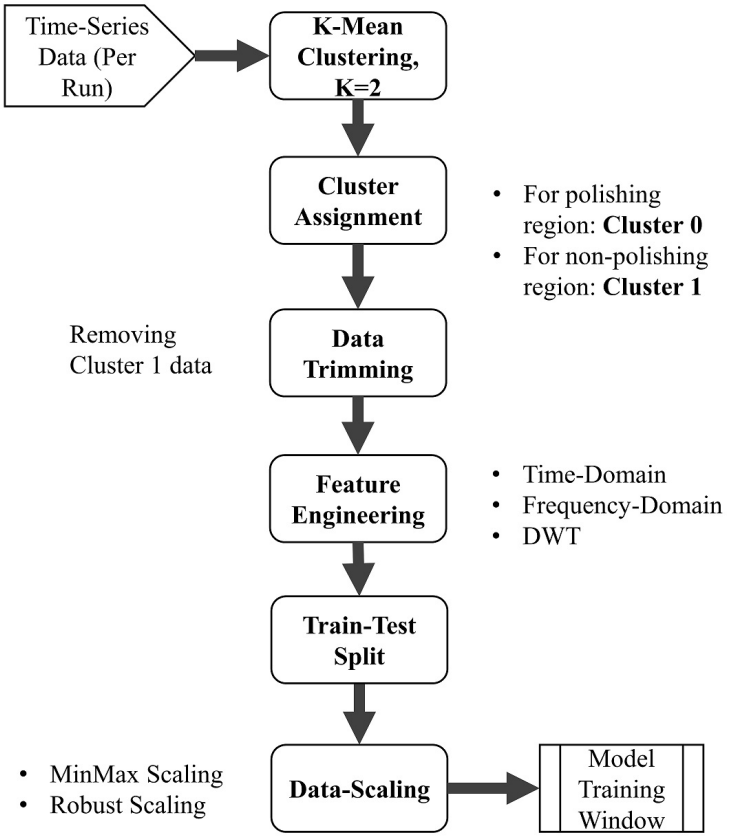

FIGURE 4.1: Block diagram of the data preprocessing pipeline.

4.1 Data Acquisition

The data used in this study was obtained from bonnet polishing experiments performed on fused silica workpieces of 100mm x 100mm dimensions. To ignore

the edge effects, a 70mm x 70mm area was selected to perform the experimentation as described in detail in [33]. A total of 34 polishing runs were conducted under varying durations and surface feed rates to introduce process diversity. The setup was equipped with six piezo-resistive load cell sensors mounted on a bespoke force table, configured to record polishing forces along all three spatial directions.

Specifically, one sensor measured force along the X-axis, two along the Y-axis, and three along the Z-axis. These multiaxial force signals were sampled at a high frequency of 500 Hz, capturing detailed temporal fluctuations in polishing forces throughout each run. Figure 4.2 shows the snippet of force signals for a single run.

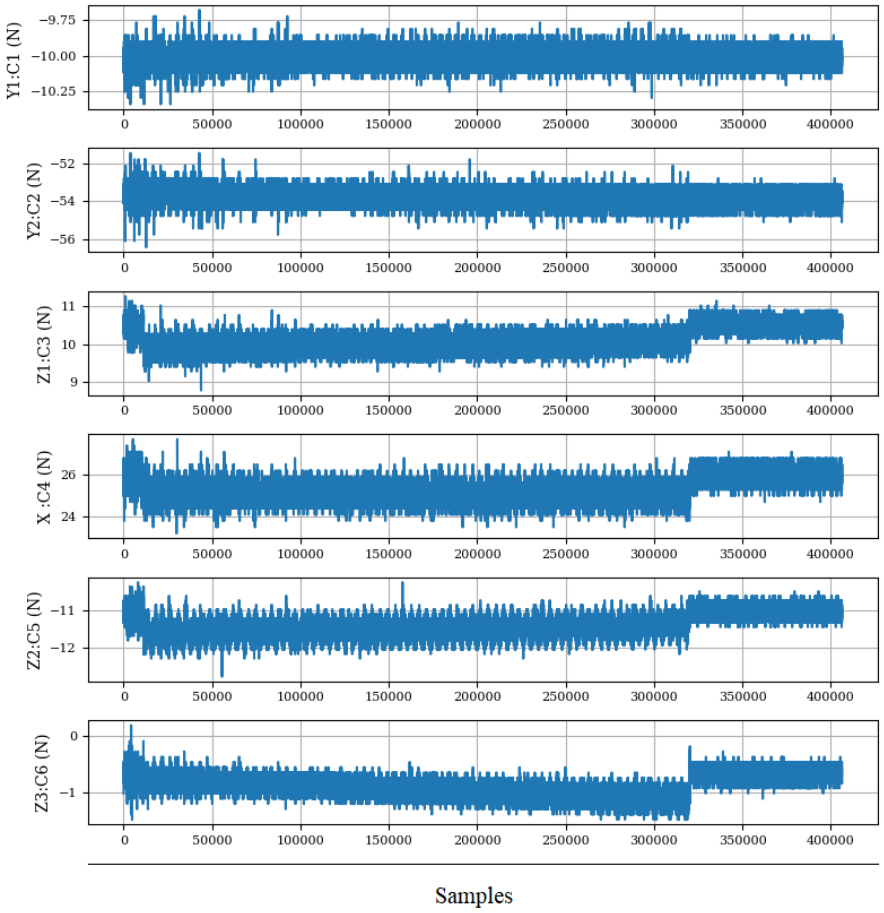

FIGURE 4.2: Raw force signals recorded from six sensors (X, Y1, Y2, Z1, Z2, Z3) during a polishing run. The signals are plotted against time to show synchronized behaviour and process variation.

In parallel with force data, two critical process parameters, slurry pH and temperature, were also recorded throughout the polishing cycle. These values were

measured in real time using sensors integrated into the slurry circulation system, sampled at a rate of 4 Hz. A representative example from a single polishing run is shown in Fig. 4.3, highlighting the evolution of these parameters over time.

As illustrated, the temperature steadily increases as the polishing process progresses. This thermal rise is attributed to frictional energy generated at the tool–workpiece interface, which is partially absorbed by the circulating slurry. The slurry acts as a thermal sink, conducting and dissipating the heat generated by the mechanical contact and abrasive interaction during material removal.

This behaviour is not only physically intuitive but also confirms the active thermal coupling between polishing dynamics and slurry condition, factors that may influence both tool performance and material removal characteristics. The pH variation, though subtler, reflects underlying changes in the slurry's chemical composition as it interacts with the workpiece surface during polishing.

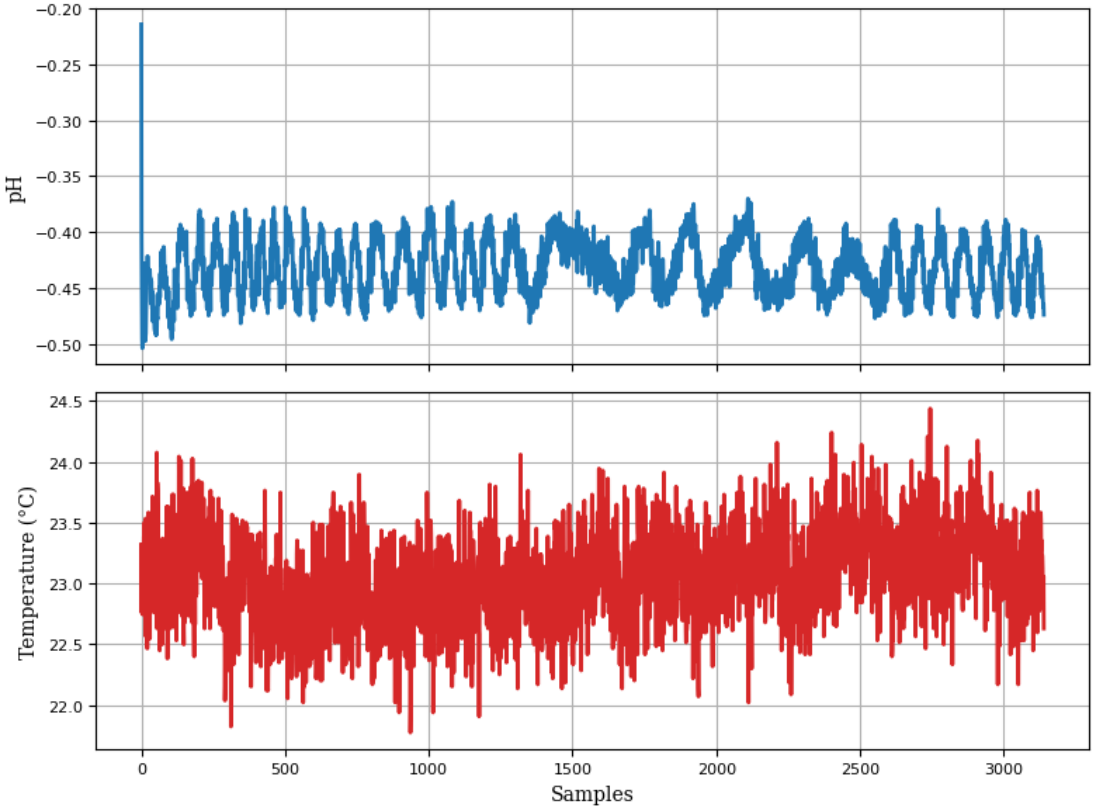

FIGURE 4.3: Real-time monitoring of slurry pH and temperature for a single polishing run. Temperature increases over time due to frictional energy transferred from the polishing interface to the slurry.

4.2 Preprocessing

Before training the predictive model, the raw data underwent several preprocessing steps to ensure its quality, relevance, and alignment. These steps included surface profile alignment and tilt correction for accurate material removal rate (MRR) computation, followed by the removal of redundant non-polishing segments in the force signals. The goal of this stage was to construct a fully automated and repeatable pipeline that could isolate only the effective polishing data while correcting for experimental variabilities.

4.2.1 Material Removal Measurement, Alignment and Tilt Correction

The accurate estimation of material removal is essential for model supervision in this study. Since the material removal rate (MRR) was not directly measured during polishing, it was computed offline using high-resolution surface profiles captured before and after each polishing run. These surface profiles were obtained using a Taylor Hobson Form Talysurf profilometer. For each run, the Z-depth after polishing was subtracted from its corresponding initial profile to derive the amount of material removed, forming the ground truth target variable for model training.

To facilitate a consistent and automated measurement pipeline, two specific modifications were introduced during the profilometry stage. A known artificial tilt of approximately 0.5 mm was deliberately added to the workpiece setup. A physical etch was made at the centre of the workpiece surface to serve as a spatial reference point. The purpose of the centre etching was to enable alignment along the lateral axis (X-direction) since no positional data or encoder feedback was available. This etching provided a consistent landmark that allowed for precise spatial matching between original and polished profiles.

Meanwhile, the intentional tilt helped simulate common misalignments caused by human error or mechanical variation in setup. It also provided an opportunity to

build a preprocessing pipeline capable of automatically identifying and correcting such deviations. As shown in Fig. 4.4, the profiles of the original and polished surfaces contain an obvious linear slope due to this introduced tilt. To remove this, a linear correction procedure was applied by fitting a line to the unpolished regions at both ends of the profile.

These areas were intentionally left unprocessed during polishing and represent the ground truth "zero-slope" reference. The fitted line's slope and intercept were then subtracted from the entire Z-profile, effectively removing the tilt and aligning both profiles to a common height baseline.

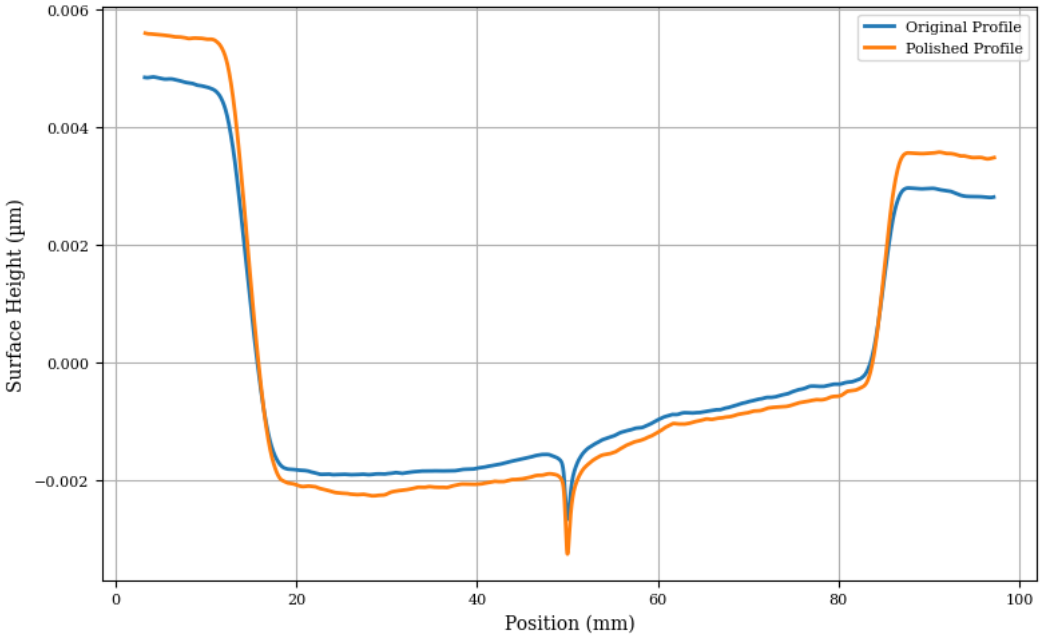

FIGURE 4.4: Surface profile of original and polished regions prior to tilt correction. A linear slope is present due to artificially introduced tilt.

After tilt correction, the material removal was computed by subtracting the Z-heights of the polished profile from those of the original. The difference represents the depth of material removed during each polishing run. The result is shown in Fig. 4.5, which includes the aligned profiles and the extracted material removal across the polished area. This approach ensures robustness and repeatability in measuring material removal, even when minor misalignments occur during experimentation. It also forms a key part of the automated data pipeline used throughout this study.

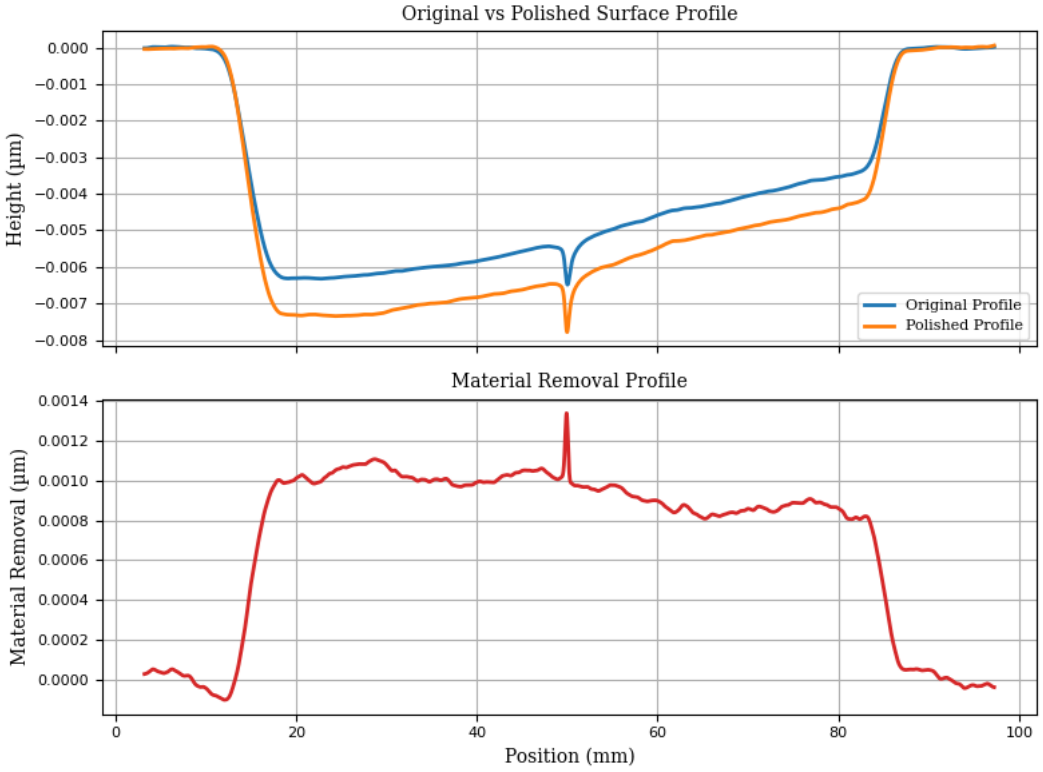

FIGURE 4.5: Original and polished surface profiles after tilt correction. Material removal is calculated by point-wise subtraction of the two profiles.

4.2.2 K-means Clustering for Non-Representative Data

Due to the manual initiation and termination of data acquisition, each polishing run included force signal segments from pre-polishing and post-polishing phases that do not contribute meaningfully to material removal behaviour. These segments, which typically contain idle or transitional tool movements, are irrelevant for model training and must be excluded. In earlier approaches, such segments were removed manually, a process that was both time-consuming and prone to inconsistencies.

To automate and standardize this task, a K-means clustering algorithm was employed to isolate the actual polishing phase from the rest of the data, as given in Fig. 4.6. The clustering was performed using the smoothed force signal from the X-axis load cell, which served as a reliable indicator due to its high sensitivity to tool engagement. Prior to clustering, a moving average filter with a window size of 40 was applied to suppress noise and stabilize the signal.

K-Means Clustering of Force Signal Segments

Require: Input folder containing raw force files; output folder for clustered data

Ensure: Clustered force data with non-polishing and polishing segments labelled

1: Define input and output folder paths
2: Create output folder if it does not exist
3: Retrieve all polishing files from input folder excluding pH & temperature files
4: Set number of clusters $k \leftarrow 2$ and moving average window size (e.g., 40)
5: **for** each file in the filtered file list **do**
6: Load tab-separated force data into a DataFrame
7: Identify all columns corresponding to force sensor readings
8: Apply moving average smoothing to each force column using the defined window size
9: Extract the X-axis force column and normalize it using standard scaling
10: Apply K-Means clustering with $k = 2$ on the normalized X-force values
11: Assign resulting cluster labels to each sample in the smoothed data
12: Append cluster labels as a new column to the DataFrame
13: Save the updated DataFrame (with cluster labels) to the output folder
14: **end for**

FIGURE 4.6: Pseudocode for K-Means clustering applied to force signal segments.

The K-means algorithm was configured to partition the signal into two distinct clusters: one representing the polishing phase and the other representing the pre- and post-polishing segments. Once the clusters were identified based on the X-axis data, the resulting labels were propagated to all six force channels to preserve temporal alignment and ensure consistent segmentation across the dataset.

An example of the clustering result from a single polishing run is shown in Fig. 4.7. The blue regions (Cluster 0) represent the active polishing phase, while the orange regions (Cluster 1) correspond to the non-polishing periods before and after.

Following clustering, the redundant segments were automatically removed, to make data read for feature extraction and model training. While the clustering itself

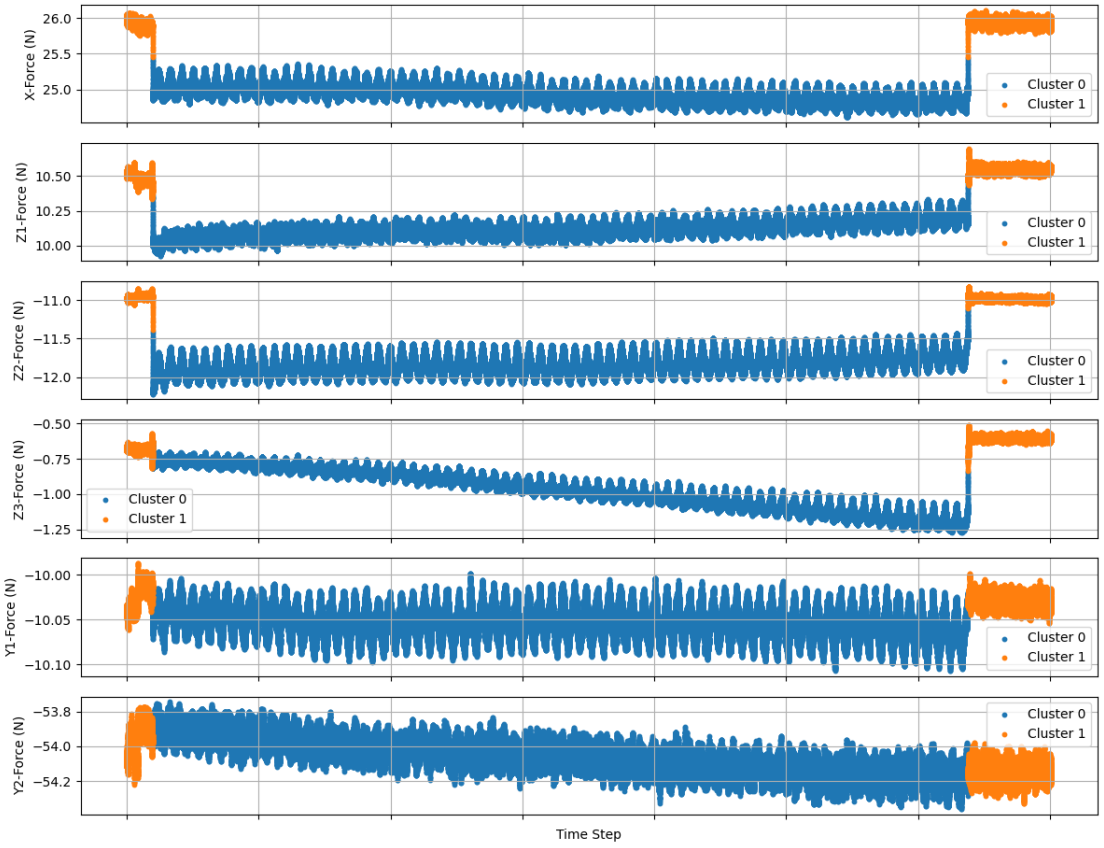

FIGURE 4.7: K-means clustering of X-axis force signal showing polishing (blue, Cluster 0) and non-polishing (orange, Cluster 1) regions for automatic data segmentation.

does not enhance model accuracy directly, it is crucial for building a robust preprocessing workflow, reducing manual intervention and improving the reliability of downstream analysis.

In conclusion, this chapter presented the basic steps required to construct a reliable and automated data pipeline for MRR prediction in bonnet polishing. Key preprocessing techniques were introduced to enhance data quality and consistency, including profile alignment, tilt correction using a central etching reference, and automated segmentation of non-polishing signal segments via K-means clustering. The outcomes of this chapter serve as a critical prerequisite for the feature engineering and modelling tasks presented in the subsequent chapters.

Chapter 5

Multi-Domain Feature Engineering and Data Exploration

This chapter focuses on multi-domain feature engineering and exploratory data analysis (EDA), forming a critical bridge between raw signal acquisition and predictive modelling. Building upon the segmented force signals obtained during preprocessing, the chapter outlines the transformation of raw time-series data into structured inputs.

A robust feature extraction pipeline was developed to capture relevant process characteristics from the time, frequency, and wavelet domains. Each domain contributes unique perspectives: time-domain features summarize signal amplitude patterns and statistical trends, frequency-domain features capture spectral characteristics and energy distribution, and wavelet-domain features provide multi-resolution insights into localized signal variations.

To evaluate the informativeness and redundancy of the extracted features, an in-depth exploratory data analysis was performed. Quantitative metrics such as Pearson correlation and distance correlation were used to identify low-impact or

redundant features, enabling dimensionality reduction without loss of predictive power.

This step ensures that only the most relevant features are retained, optimizing the input space for downstream learning tasks. As indicated in the preprocessing pipeline shown in Fig. 4.1, this chapter continues the second half of the preprocessing workflow by focusing on domain feature extraction and data exploration. Overall, this chapter establishes a structured and analytically justified foundation for developing accurate and generalizable models for material removal rate (MRR) prediction.

5.1 Feature Engineering

For each polishing run, the preprocessed force signals were segmented into 141 equal-length bins, corresponding to the 141 spatial tool-path steps. This segmentation enabled localized analysis of the polishing behaviour, facilitating fine-grained learning of spatially varying material removal patterns. Within each segment, the following feature types were extracted:

5.1.1 Time-Domain (TD) Features

Time-domain features describe the statistical properties of the force signal in the temporal domain. These include:

5.1.1.1 Mean

Represents the average force applied during the segment:

$$\mu = \frac{1}{N} \sum_{i=1}^{N} x_i \tag{5.1}$$

5.1.1.2 Standard Deviation (StdDev)

Measures the variability from the mean:

$$\sigma = \sqrt{\frac{1}{N}\sum_{i=1}^{N}(x_i - \mu)^2} \tag{5.2}$$

5.1.1.3 Root Mean Square (RMS)

Emphasizes the effective magnitude:

$$\text{RMS} = \sqrt{\frac{1}{N}\sum_{i=1}^{N}x_i^2} \tag{5.3}$$

5.1.1.4 Skewness

Indicates the asymmetry of the signal distribution:

$$\text{Skewness} = \frac{1}{N}\sum_{i=1}^{N}\left(\frac{x_i - \mu}{\sigma}\right)^3 \tag{5.4}$$

5.1.1.5 Kurtosis

Evaluates the peakedness or tail heaviness:

$$\text{Kurtosis} = \frac{1}{N}\sum_{i=1}^{N}\left(\frac{x_i - \mu}{\sigma}\right)^4 \tag{5.5}$$

These statistical indicators capture the general behaviour of forces applied at each polishing step, including magnitude, stability, and signal shape.

5.1.2 Frequency-Domain (FD) Features

Frequency-domain features were derived from the Power Spectral Density (PSD) of each segment using Welch's method. These features help quantify the periodic content and spectral energy of the signal.

5.1.2.1 Spectral Energy

Total power in the frequency domain:

$$E = \sum_{k=1}^{M} P_k \tag{5.6}$$

where P_k is the PSD at frequency bin k.

5.1.2.2 Spectral Entropy

Measures the irregularity or disorder of the spectrum:

$$H = -\sum_{k=1}^{M} P_k \log(P_k + \epsilon) \tag{5.7}$$

where ϵ is a small constant for numerical stability.

These FD metrics highlight the vibrational characteristics and randomness of the polishing forces, often linked to tool-workpiece interaction dynamics.

5.1.3 Discrete Wavelet Transform (DWT) Feature

To capture localized time-frequency characteristics, a single-level Discrete Wavelet Transform (DWT) was applied using the Daubechies 4 (db4) mother wavelet. Only the approximation coefficients, which represent the low-frequency content, were retained.

Approximation coefficient mean describes the smooth structural trend:

$$\mu_{A_j} = \frac{1}{N} \sum_{i=1}^{N} A_j(i) \tag{5.8}$$

where $A_j(i)$ denotes the approximation coefficient at level j.

These coefficients encode long-term force trends and filter out high-frequency noise, capturing macro-level polishing behaviours.

The combined feature set, spanning statistical (TD), spectral (FD), and localized wavelet (DWT) domain, provides a comprehensive representation of the force signals. TD features offer magnitude and distributional context; FD features uncover the energy and chaos in polishing; DWT features retain localized structural information. This multi-domain representation equips the MARCNN architecture with rich, hierarchical input patterns that improve prediction of the material removal rate at each spatial location.

The complete multi-domain feature extraction process including time-domain, frequency-domain, and wavelet-based metrics for each polishing segment is outlined in Fig. 5.1. This algorithm was applied to clustered and segmented force data for each polishing run to generate a comprehensive feature matrix used for model training.

5.2 Exploratory Data Analysis (EDA)

To understand the underlying relationships between input features and the material removal rate (MRR), a series of exploratory data analyses were conducted.

The primary goal was to evaluate the strength and nature (linear or non-linear) of associations between the sensor-derived features and the target output (MRR), and to identify the most informative signals and feature groups for model development.

Multi-Domain Feature Extraction from Clustered Force Data

Require: Clustered force data files from six sensors
Ensure: Feature matrix with TD, FD, and DWT features for each segment

for all files in `Clustered_run_*.csv` **do**
  Load force signal data as `df`
  Remove rows with `Cluster Label = 1`
  Drop `Cluster Label` and `Timestamp` columns
  Split data into 141 equal-length segments
  for all segments s_i in signal **do**
    if s_i is not empty **then**
      for all force channels in s_i **do**
        Time-Domain Features: Compute Mean, StdDev, RMS, Skewness, Kurtosis
        Frequency-Domain Features: Compute PSD → Spectral Energy, Entropy
        DWT Feature: Compute Approximation Coefficient Mean (db4)
      end for
    end if
  end for
end for
Save all extracted features to a CSV file

FIGURE 5.1: Procedure for multi-domain feature extraction from clustered force data.

5.2.1 Linear Correlation

Initially, Pearson correlation coefficients were computed between the mean force values from all six sensors and their corresponding MRR values. As shown in Fig. 5.2, the correlation matrix highlights weak or negligible linear correlations across all force channels. This outcome suggests that simple linear dependencies between mean forces and MRR are limited in this complex polishing environment. Therefore, Pearson correlation may be insufficient for capturing the deeper, potentially non-linear interactions governing the material removal behaviour.

5.2.2 Non-linear Dependency via Distance Correlation

To overcome the limitations of linear correlation analysis, distance correlation was employed to reveal both linear and non-linear dependencies. Unlike Pearson

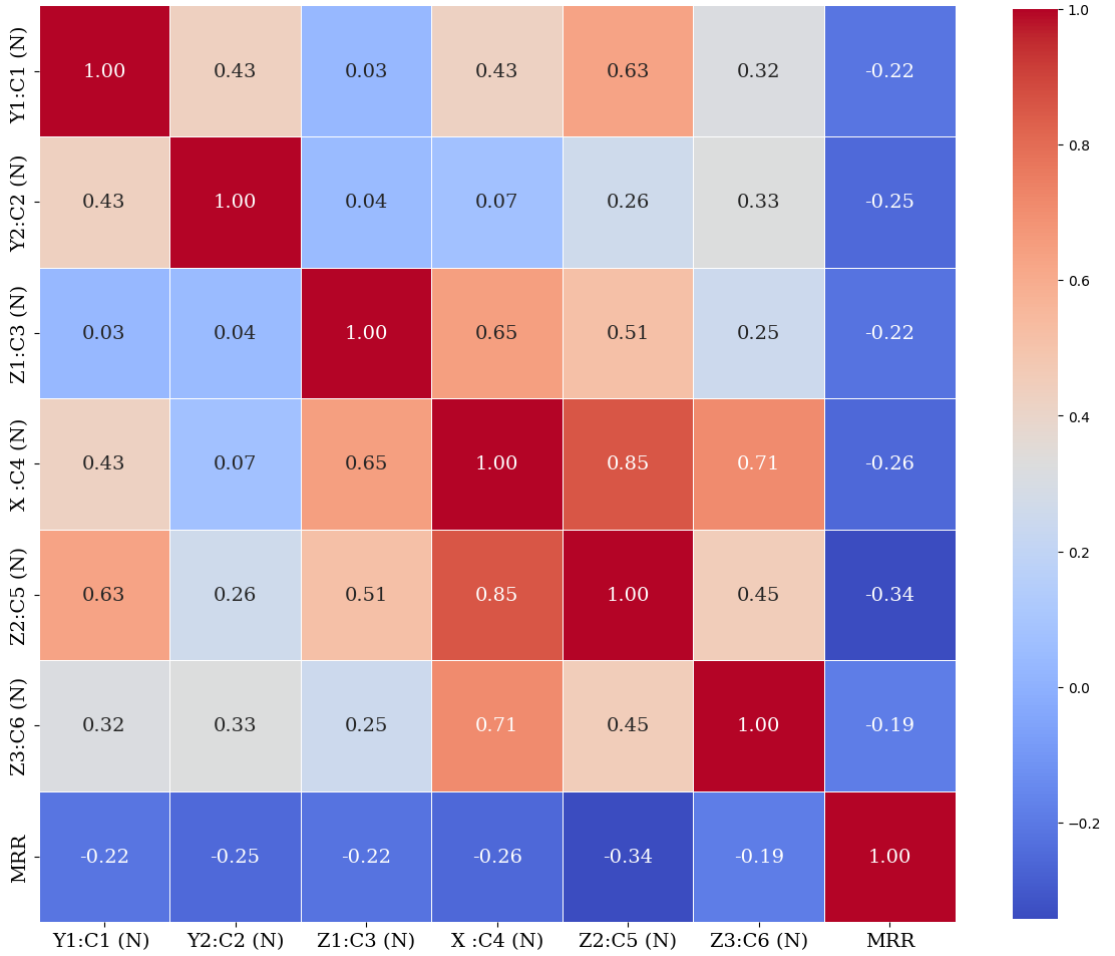

FIGURE 5.2: Pearson correlation matrix between mean forces and MRR.

correlation, distance correlation can detect any statistical dependence, regardless of functional form.

The resulting analysis, shown in Fig. 5.3, revealed significantly higher correlation values, particularly for Z-axis force signals, which represent normal polishing forces. These forces are fundamentally responsible for tool pressure during polishing, thus exhibiting strong relationships with material removal.

5.2.3 Cumulative Feature Group Correlation with MRR

To assess which groups of features were collectively most informative, cumulative distance correlations were computed for each domain: Time-Domain (TD), Frequency-Domain (FD), and Discrete Wavelet Transform (DWT), along with the

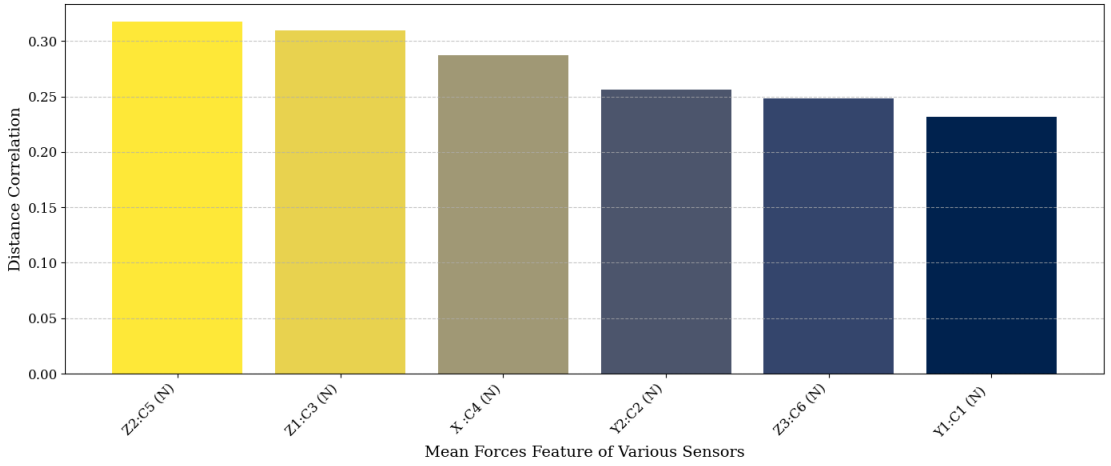

FIGURE 5.3: Distance correlation of mean forces with MRR.

average change in slurry pH and temperature. As visualized in Fig. 5.4, FD features had the highest overall correlation with MRR, followed by temperature, TD features, pH, and finally DWT features.

This suggests that spectral features such as energy and entropy are more strongly associated with material removal behaviour, potentially due to their sensitivity to oscillatory force dynamics and polishing-induced vibration.

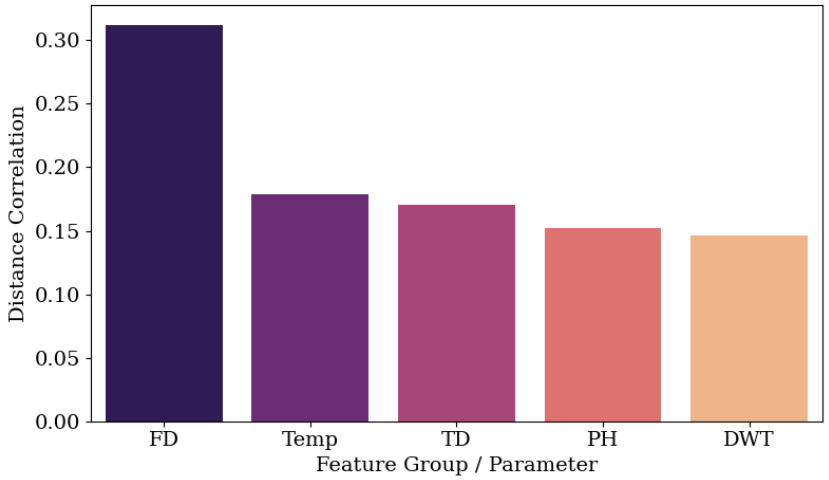

FIGURE 5.4: Cumulative distance correlation of TD, FD, DWT, pH, and temperature features with MRR.

5.2.4 Sensor-wise Feature Correlation

To further refine the analysis, domain-wise features from each individual sensor were evaluated to determine their sensor-specific importance in predicting MRR. In this context, TD, FD, and DWT features were aggregated per sensor, and their cumulative distance correlation scores with MRR were computed. As illustrated in Fig. 5.5, the Y2:C2 sensor, associated with tangential or frictional force, showed the highest cumulative correlation, followed by Z2:C5 and Z1:C3, which represent vertical or normal forces.

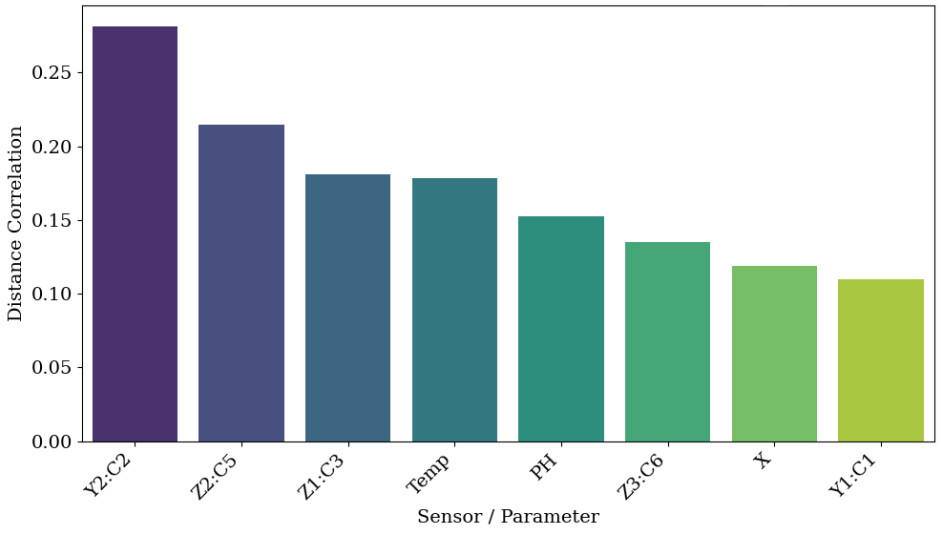

FIGURE 5.5: Sensor-wise cumulative distance correlation of domain features along with pH and temperature with MRR.

These results align well with physical polishing dynamics, where both friction and pressure are primary contributors to material removal. Additionally, temperature also showed a significant correlation, likely due to its role in indicating energy transfer from the surface during polishing. In contrast, pH exhibited relatively lower correlation but remained non-negligible, indicating secondary but meaningful influence.

This chapter established a comprehensive feature engineering and exploratory data analysis framework to transform raw, segmented force signals into structured, informative inputs for machine learning models. By extracting features from the

time, frequency, and wavelet domains, the study ensured a multi-domain representation of the polishing process forces, capturing both global trends and localized variations. The exploratory data analysis revealed valuable insights into the predictive relevance of different feature domains and sensor channels.

While Pearson correlation exposed limited linear relationships, distance correlation successfully identified non-linear dependencies, particularly highlighting the importance of normal (Z-axis) and tangential (Y-axis) forces. Among feature domains, frequency-domain metrics demonstrated the strongest overall association with MRR, emphasizing their utility in characterizing oscillatory and dynamic polishing behaviours. Additionally, sensor-wise analysis confirmed that certain force channels, especially Y2 and Z2, consistently provided more informative signals for MRR prediction. These findings guided the subsequent modelling efforts. Overall, this chapter provided a robust analytical foundation, ensuring that only high-value, interpretable features were forwarded into the learning architecture described in the following chapter.

Chapter 6

Machine Learning Model Development for MRR Prediction

This chapter elaborates the model architecture employed to improve the prediction accuracy of Material Removal Rate (MRR) in the bonnet polishing process. A hybrid deep feature fusion learning architecture was developed that combines the strengths of both Artificial Neural Networks (ANN) and a Multi-Branch Residual Convolutional Neural Network (MARCNN). This design enables the model to exploit both global statistical summaries and localized, domain-rich patterns from multi-modal sensor data.

The ANN branch utilizes mean features, representing aggregated force sensor values, capturing broad trends across the polishing process. Meanwhile, the MARCNN processes time-series derived features across multiple signal domains (Time-Domain, Frequency-Domain, and Discrete Wavelet Transform), alongside slurry-related environmental conditions (pH and temperature). By structurally isolating simple mean inputs from complex feature sets, each branch is able to learn efficiently within its optimal regime. The outputs of both branches are fused at a later stage to produce an integrated and accurate regression output for MRR. This deep feature fusion architecture not only enhances predictive performance but also contributes to model robustness and interpretability. Figure 6.1 summarizes the entire solution pipeline, bringing together the automated preprocessing

steps, multi-domain feature extraction, and the final predictive model architectures developed in this chapter.

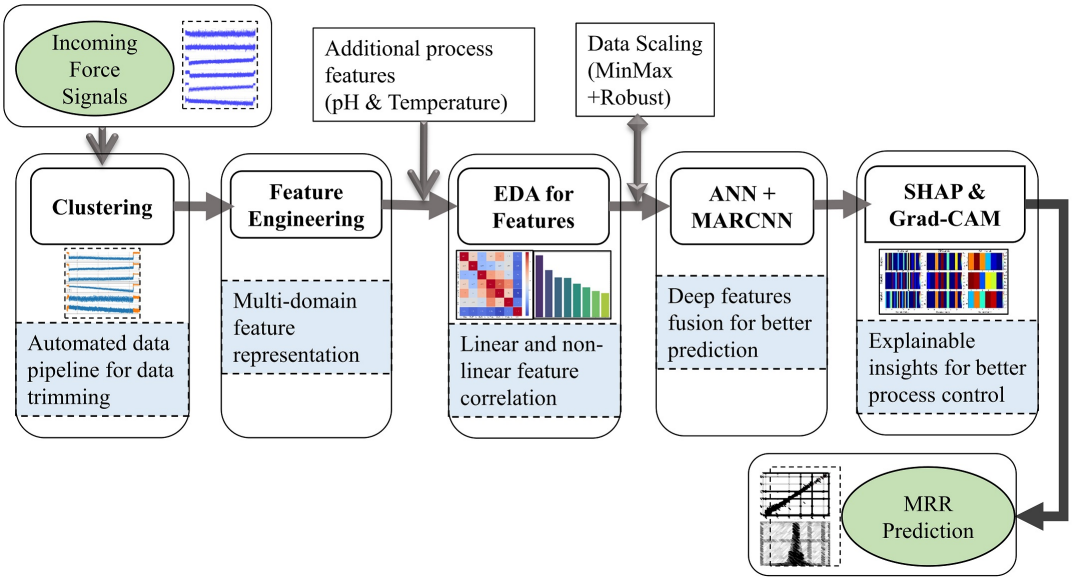

FIGURE 6.1: Complete block diagram of the proposed automated framework for MRR prediction.

6.1 Artificial Neural Network (ANN) Branch

The ANN branch of the deep feature fusion model was dedicated to processing six mean force features, each representing the average force captured from one of the piezo-resistive load cell sensors during polishing. These mean features act as concise indicators of overall force magnitude, offering a simplified yet informative snapshot of the polishing dynamics.

This ANN architecture follows the structure proposed in a previous study [66], consisting of three fully connected layers with 10, 60, and 10 neurons, respectively. Each layer employs the ReLU activation function and applies L2 regularization to mitigate over-fitting. The model was trained using the Adam optimizer, with early stopping and learning rate reduction on validation loss plateau as part of the training strategy.

The dataset was split into training (60%), validation (20%), and test (20%) subsets to ensure robust generalization assessment. Although relatively lightweight, this branch contributes essential global trends that may be overlooked in localized signal analysis.

6.2 Multi-Branch Residual CNN With Attention (MARCNN)

To handle the more complex and granular signal-derived features, a dedicated convolutional neural network (CNN) was designed. This branch incorporates four parallel input streams, each tailored to a specific type of feature: Time-Domain (TD), Frequency-Domain (FD), Discrete Wavelet Transform (DWT), and environmental conditions (slurry pH and temperature). These feature sets represent different perspectives on the polishing process, from statistical variability to spectral content and system state, enabling the model to learn nuanced relationships between signal behaviour and material removal outcomes.

An overview of the MARCNN architecture is illustrated in Fig. 6.2. Each feature group is processed through its own independent sub-branch consisting of the following components:

- Two sequential 1D convolutional layers (32 and 64 filters, kernel size = 3, ReLU activation) for local pattern extraction.
- Residual skip connections to mitigate vanishing gradients and improve convergence stability.
- Batch Normalization layers for faster and more stable training.
- A custom attention mechanism to highlight the most relevant temporal or spectral patterns within each feature branch.
- Flattening layers followed by Dropout (rate = 0.3) to convert 2D maps into vector representations and prevent over-fitting.

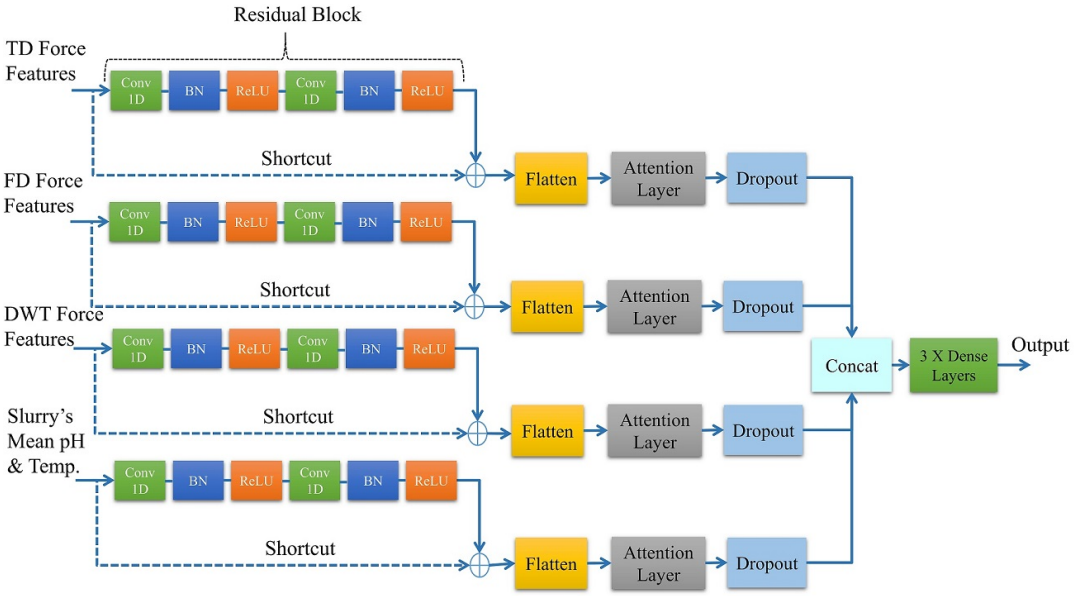

FIGURE 6.2: Architecture of the MARCNN model showing four parallel input branches (TD, FD, DWT, and PH/Temp), each with residual and attention mechanisms.

Each branch feeds into a shared dense network with three fully connected layers of 80 neurons each, activated via Swish functions. This allows the model to integrate feature representations across different domains. The final output layer uses linear activation to regress the predicted MRR value.

Importantly, the penultimate dense layer of the MARCNN acts as a feature embedding layer, producing a high-level abstract representation of the multi-domain inputs. This embedding is concatenated with the output of the ANN branch to form a unified input to the final deep feature fusion layer, where both global and localized signals are merged for final prediction. The complete training and evaluation pipeline of the MARCNN model, including data preprocessing, multi-branch input processing, residual and attention mechanisms, and performance-based model saving, is formally outlined in Fig. 6.3.

6.2.1 Addressing Overfitting Risk in MARCNN

To mitigate overfitting in the proposed MARCNN architecture, several regularization and generalization strategies were employed during model training. Firstly,

Training Procedure for MARCNN Model

Require: TD, FD, DWT, and PH/Temp features; corresponding MRR values
Ensure: Trained MARCNN model and evaluation metrics

Preprocessing:
    Apply **RobustScaler** followed by **MinMaxScaler** to all input features
    Scale target MRR using **MinMaxScaler**
Split dataset into training and testing sets
Define Attention Layer:
    Apply Dense layer with GELU activation
    Apply another Dense layer with Softmax to compute attention scores
    Multiply input with scores to generate attention-weighted output
Define Residual Block:
    Apply two Conv1D layers (kernel sizes 5 and 3) with ReLU activation
    Apply Batch Normalization after each Conv1D
    Add shortcut via 1x1 Conv1D connection
Build MARCNN Model:
    Apply residual block, then flatten the output
    Apply attention and dropout layers
    Concatenate all branch outputs
    Apply three Dense layers (80 neurons each, Swish activation)
    Apply final Dense layer with 1 neuron and linear activation
Compile model with Adam optimizer, MSE loss, and MAE metric
Train Model (10 Runs):
for each experimental run **do**
    Use **ModelCheckpoint** to save best model (min val_MAE)
    Use **ReduceLROnPlateau** to adjust learning rate on plateau
    Use **EarlyStopping** to stop training if no improvement
    Train for up to 500 epochs using validation split
    Save best model if current MAE is lowest
end for

FIGURE 6.3: Workflow of the MARCNN model training procedure.

early stopping was implemented to monitor validation loss and halt training once performance plateaued, preventing unnecessary epochs that could lead to overfitting. Additionally, dropout layers were introduced after key convolutional blocks within each branch of the MARCNN to randomly deactivate a fraction of neurons during training, thereby reducing reliance on specific feature patterns and promoting generalization. Batch normalization was also used to stabilize and accelerate convergence while providing a slight regularization effect. Finally, the training dataset was split using stratified sampling to ensure consistent representation of the polishing conditions across training and validation subsets, reducing

bias. Collectively, these techniques ensured that the MARCNN model maintained high predictive performance without overfitting to the training data.

6.3 Deep Feature Fusion Technique

To harness the complementary strengths of both global statistical summaries and localized temporal-spectral representations, a deep feature fusion network was designed by integrating two specialized sub-networks: an Artificial Neural Network (ANN) and a Multi-Branch Residual Convolutional Neural Network with attention mechanism (MARCNN).

The ANN branch, operating on global mean features derived from six force sensors, captures broad trends in the polishing force behaviour. In contrast, the MARCNN processes temporally segmented and domain-specific features (TD, FD, DWT) alongside environmental variables such as slurry pH change and temperature, which are critical for modelling localized and non-linear dynamics.

The deep feature fusion architecture is formed by concatenating the feature embeddings from the penultimate dense layers of both branches. This fused representation captures high-level abstractions from the MARCNN and compact statistical summaries from the ANN, offering a comprehensive feature space for final prediction. This combined embedding is passed through a fully connected layer with 16 neurons using the hyperbolic tangent (tanh) activation function, followed by a final output layer with a ReLU activation to predict the Material Removal Rate (MRR).

The complete set of architectural and training parameters used in the deep feature fusion strategy is summarized in Table 6.1. This fusion strategy allows the model to capture both macro-scale process behaviour and micro-scale signal dynamics, improving robustness and overall predictive performance. Comparative evaluations demonstrated that the deep feature fusion technique consistently outperformed its individual components (ANN-only or MARCNN-only), validating

TABLE 6.1: Parameters of the Hybrid Deep Feature Fusion Network

Component	**Configuration**
ANN Branch	3 Dense layers (10, 60, 10 neurons), ReLU activation, L2 regularization
MARCNN Branch (Each Stream)	2 Conv1D layers (32, 64 filters, kernel size 3), Residual connection, BatchNorm, Attention, Dropout (0.3), Flatten
MARCNN Output Layers	3 Dense layers (80 neurons), Swish activation
Fusion Layer	Dense layer (16 neurons), tanh activation
Final Output Layer	Dense layer (1 neuron), ReLU activation
Optimizer	Adam
Loss Function	Mean Squared Error (MSE)
Evaluation Metric	Mean Absolute Error (MAE)
Regularization	L2 on ANN branch; Dropout in MARCNN branches
Learning Strategy	ReduceLROnPlateau, EarlyStopping on validation loss

the efficacy of integrating multi-modal and multi-scale information sources in polishing process modelling.

6.4 Evaluation Metrics

To quantitatively assess the performance of the proposed models, three standard regression metrics were employed: Mean Absolute Error (MAE), Root Mean Squared Error (RMSE), and the Coefficient of Determination (R^2).

These metrics offer complementary perspectives on the model's accuracy, sensitivity to outliers, and explanatory power.

6.4.1 Mean Absolute Error (MAE)

Measures the average absolute difference between predicted and true MRR values.

$$\text{MAE} = \frac{1}{n}\sum_{i=1}^{n}|y_i - \hat{y}_i| \tag{6.1}$$

6.4.2 Root Mean Squared Error (RMSE)

Emphasizes larger prediction errors by squaring the residuals before averaging.

$$\text{RMSE} = \sqrt{\frac{1}{n}\sum_{i=1}^{n}(y_i - \hat{y}_i)^2} \tag{6.2}$$

6.4.3 Coefficient of Determination ($\mathbf{R^2}$)

Represents the proportion of variance in the actual MRR that is captured by the model.

$$R^2 = 1 - \frac{\sum_{i=1}^{n}(y_i - \hat{y}_i)^2}{\sum_{i=1}^{n}(y_i - \bar{y})^2} \tag{6.3}$$

Here, y_i and $\hat{y}_i$ denote the actual and predicted MRR values respectively, $\bar{y}$ is the mean of the actual values, and n is the number of samples. Together, these metrics provide a comprehensive evaluation of the model's predictive quality in both average-case and worst-case scenarios.

In summary, this chapter presented the architectures for baseline (ANN) model, a more advanced model (MARCNN) and deep feature fusion using both to achieve superior predictive performance. Deep feature fusion achieves better results by combining an ANN for mean statistical features and a MARCNN for richer temporal and spectral representations. The integration of these diverse inputs was designed to exploit both global and localized patterns in the polishing process. The next chapter presents a thorough evaluation of the proposed approach, including ablation studies and performance comparisons with baseline models.

Chapter 7

Results and Discussion

This chapter presents a detailed evaluation of the proposed deep feature fusion technique designed to predict Material Removal Rate (MRR) in the bonnet polishing process using multi-source sensor data. The predictive performance of the deep feature fusion framework is systematically compared against two baseline models: a stand-alone Artificial Neural Network (ANN) and a Convolutional Neural Network (CNN). The ANN model, which is adapted from earlier work [66], processes mean force values and serves as the foundational reference. The CNN model, by contrast, is designed to learn richer temporal patterns from segmented, multi-domain features including time-domain (TD), frequency-domain (FD), and discrete wavelet transform (DWT) representations.

Although the ANN model was retrained using the newly preprocessed dataset, refined through automated clustering and segmentation, it continued to demonstrate performance metrics consistent with those reported in prior studies. This consistency validates the robustness of the ANN-based approach and highlights the benefit of transitioning from manual to automated preprocessing, thereby enhancing scalability and reproducibility.

To exploit the complementary strengths of both global statistical summaries and localized temporal features, a deep feature fusion architecture was proposed, integrating the ANN and CNN outputs into a unified prediction framework. This

architecture is expected to improve generalization by simultaneously capturing macro-level trends and micro-level dynamics of the polishing process. The subsequent sections provide a comprehensive analysis of model performance, including comparative evaluation, ablation experiments, and model interpretability through explainability techniques.

7.1 Results on Testing Data

To evaluate the effectiveness of the proposed modelling framework for MRR prediction, three distinct neural architectures were compared: a baseline Artificial Neural Network (ANN), a multi-branch Convolutional Neural Network (CNN), and a hybrid deep feature fusion architecture combining both ANN and CNN outputs. Each model was trained and tested using a standardized dataset processed through the proposed automated pipeline, which included clustering-based segmentation and sensor signal alignment, to ensure fairness and consistency across evaluations.

TABLE 7.1: Performance Comparison of ANN, CNN (without pH & Temp), and Deep Feature Fusion Network

Model	**MAE (μm)**	**R^2 Score**	**RMSE**
ANN [66]	0.0713	0.9854	0.1373
MARCNN (without pH & Temp)	0.0680	0.9772	0.1719
Deep Feature Fusion	**0.0563**	**0.9881**	**0.1239**

The ANN model served as the reference architecture, relying solely on mean force features computed across each segmented tool path. This choice reflects the assumption that global statistical trends, such as average load levels, correlate with overall material removal behaviour. The model achieved strong results with an R^2 score of 0.9854 and a mean absolute error (MAE) of 0.0713 μm. Importantly, despite the model being retrained on data refined through automated clustering and segmentation, its performance remained consistent with earlier results reported in

literature [66]. It showed that the clustering for data segmentation has no effects on results.

Clustering for data segmentation just automated the laborious task of finding out the regions of no polishing zones and removing them from training data. This reinforces the robustness of mean-based statistical models in capturing macro-level trends, especially when supported by carefully engineered preprocessing steps that preserve signal integrity.

The MARCNN model was introduced to capture localized, step-wise patterns in the polishing process that are not accessible through global statistics alone. Structured as a multi-branch architecture, this model processes features across three domains: time-domain (TD), frequency-domain (FD), and discrete wavelet transform (DWT). Each branch extracts hierarchical representations from these inputs using residual blocks and attention mechanisms.

The reported results correspond to a version excluding pH and temperature features, as they show a slight increment in results. This finding discussed further in detail in Section 7.5. The MARCNN, trained without pH and Temperature data, achieved an MAE of 0.0680 μm and an R^2 of 0.9772, validating its ability to model more complex, dynamic relationships. However, a slight increase in RMSE (0.1719) compared to the ANN suggests that while MARCNN captures local variations better, it may be more sensitive to outliers or overfitting in the absence of global summaries.

The deep feature fusion architecture, which integrates the ANN and MARCNN branches by concatenating their penultimate layer outputs before final regression, yielded the best overall results across all metrics: an MAE of 0.0563 μm, an RMSE of 0.1239, and an R^2 score of 0.9881. These outcomes indicate a synergistic effect, the statistical insight from ANN complements the fine-grained temporal representations learned by the MARCNN. From an engineering standpoint, this fusion addresses a key challenge in polishing process modelling: the non-linear interplay between macro-level process stability and micro-level force variations. The deep feature fusion architecture's superior performance demonstrates that combining

domain-specific statistical summaries with deep representations of localized signal behaviour leads to more accurate, robust, and generalizable predictions.

7.2 Results on Training Data

Following the evaluation on the test dataset, the training results of the models are presented in Table 7.2. This allows for a comprehensive understanding of each model's learning capability and generalization by comparing performance across both training and testing phases. The results are reported using the same evaluation metrics: Coefficient of Determination (R^2), Root Mean Squared Error (RMSE), and Mean Absolute Error (MAE).

TABLE 7.2: Model Performance on Training Data

Model	**R^2 Score**	**RMSE (µm)**	**MAE (µm)**
ANN [66]	0.9947	0.0846	0.0491
MARCNN (CNN)	0.9949	0.0833	0.0344
Deep Feature Fusion	**0.9972**	**0.0616**	**0.0339**

The results indicate that all models perform very well in the training data, achieving R^2 scores greater than 0.99, which means an excellent model fit. The ANN model demonstrates solid predictive capability, though with slightly higher error values due to its simpler, fully connected architecture. The MARCNN model benefits from its ability to extract deep, domain-specific patterns through residual connections and attention layers, leading to improved accuracy over the ANN. The deep feature fusion outperforms both individual models on all training metrics, achieving the lowest MAE and RMSE, and the highest R^2. This highlights the effectiveness of combining the statistical ANN features with the deep multi-branch feature learning of the MARCNN.

When comparing these results with the performance of the test set previously discussed, a slight increase in RMSE and MAE is observed, as expected. However,

the consistency between training and testing metrics, especially in the deep feature fusion, suggests that the model has not over-fitted the training data. The ability of the deep feature fusion to generalize effectively while maintaining high accuracy validates the robustness of the proposed framework for predicting the real-world material removal rate (MRR).

7.3 Model Prediction Analysis and Residual Distribution

To complement the quantitative metrics for testing dataset discussed previously, a detailed diagnostic analysis was conducted to assess the predictive behaviour and statistical integrity of the deep feature fusion technique. This section presents a series of visualizations including prediction alignment plots, residual diagnostics, and error distribution analyses, all aimed at verifying the model's robustness, generalization capacity, and suitability for real-world deployment in precision polishing processes.

7.3.1 Actual vs. Predicted MRR on Testing Set

The results highlighted in the evaluation tables suggest the improved prediction performance of the deep feature fusion technique on validation dataset. For further verification of the predicted results of validation set a plot for actual vs. predicted MRR values on validation data is presented. Figure 7.1 shows the scatter plot of predicted versus actual MRR values obtained on the test set. The close clustering of points along the $y = x$ reference line indicates a high degree of predictive fidelity and minimal bias. Importantly, the model maintains its accuracy across the full range of MRR magnitudes, demonstrating both generalizability and reliability in predicting subtle and substantial material removal patterns alike. Such alignment is critical in polishing applications, where over or under removal of material can compromise surface quality and form accuracy.

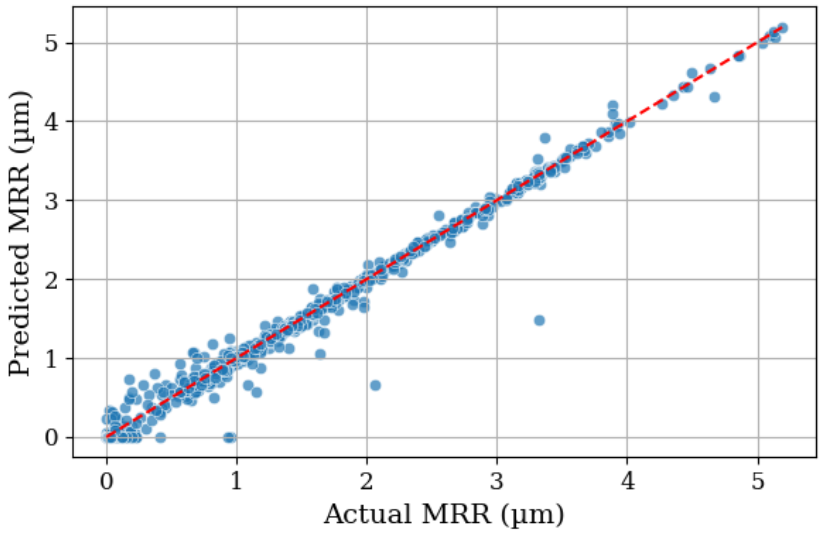

FIGURE 7.1: Scatter plot of actual vs. predicted MRR values. The red dashed line represents the ideal $y = x$ relationship.

To further verify the model's statistical alignment, Kernel Density Estimation (KDE) curves of the predicted and actual MRR distributions are plotted in Fig. 7.2. The predicted distribution tracks the actual distribution remarkably well across the domain. This indicates that the model is not only accurate in individual predictions but also in reproducing the global statistical characteristics of the target variable. Such fidelity is essential for ensuring consistent performance across batch production scenarios or extended polishing cycles.

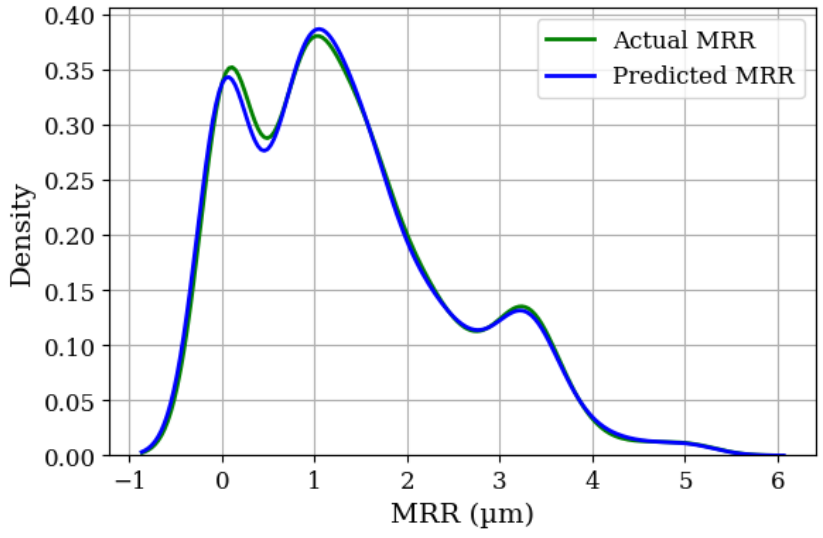

FIGURE 7.2: Kernel Density Estimation (KDE) curves comparing actual and predicted MRR distributions.

7.3.2 Residual and Error Distribution Analysis

Figure 7.3 depicts the residuals, defined as the difference between the actual and predicted values, plotted against the predicted MRR. The residuals are symmetrically dispersed around zero and show no discernible trends or heteroscedastic patterns. This uniform scatter indicates that the model's errors are independent of the magnitude of the predicted value, satisfying key assumptions of homogeneity of variance in regression modelling. Such behaviour enhances confidence in the model's deployment across varying polishing conditions and material batches.

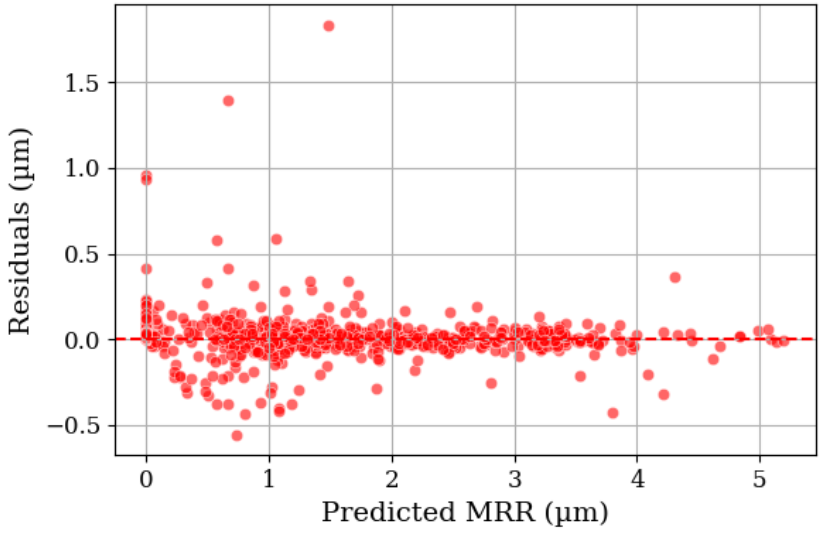

FIGURE 7.3: Residual plot showing prediction errors as a function of predicted MRR. The red line denotes the zero-error axis.

The residual histogram in Fig. 7.4 shows a sharply peaked and nearly symmetrical distribution centred around zero. The shape approximates a Gaussian curve, further confirming the absence of systematic bias or skewed prediction behaviour. From an engineering standpoint, this reflects a stable and unbiased estimator, capable of maintaining predictive integrity across process noise and minor fluctuations.

Finally, the histogram of absolute prediction errors in Fig. 7.5 underscores the model's precision. Most samples exhibit absolute errors clustered near zero, with very few outliers. This confirms that the deep feature fusion technique not only reduces average error but also maintains a narrow distribution of errors, a critical

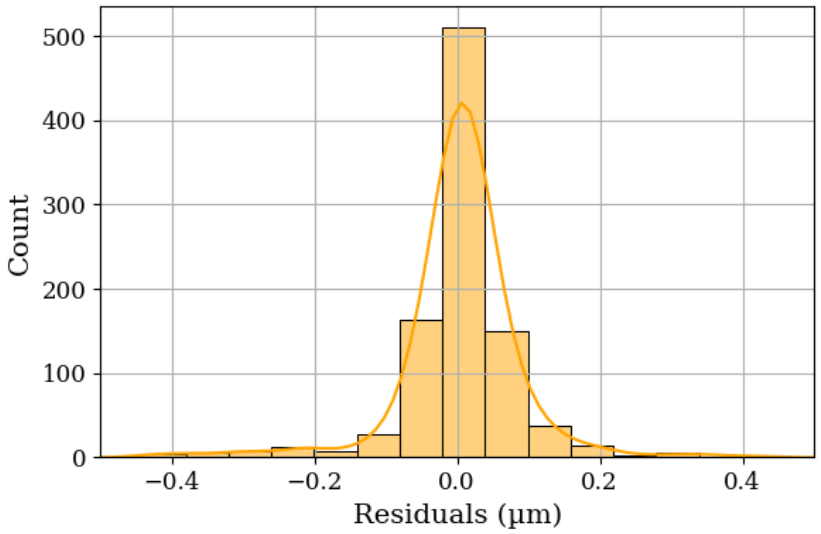

FIGURE 7.4: Histogram of residuals with KDE overlay, approximating a normal distribution centred near zero.

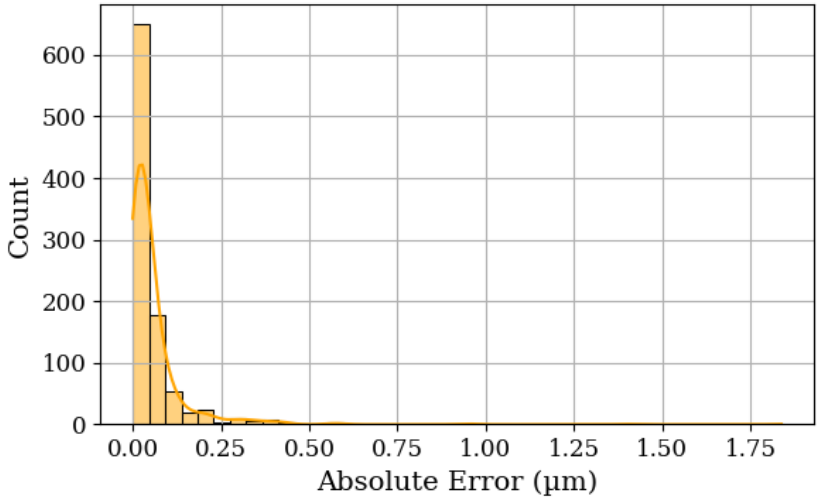

FIGURE 7.5: Histogram of absolute prediction errors. The distribution is sharply skewed toward low-error regions.

requirement for high-precision polishing tasks where tolerance bands are often tight.

Collectively, the diagnostic plots validate the predictive consistency and structural reliability of the deep feature fusion technique. The close agreement between actual and predicted distributions, combined with well-behaved residuals and low-error magnitudes, reflect a mature model architecture. These characteristics are crucial in real-world manufacturing environments, where prediction stability and precision

are non-negotiable for achieving desired surface finish and form accuracy.

7.4 Explainability Analysis of the Proposed Model (XAI)

To enhance transparency and interpretability of the proposed deep feature fusion learning framework, explainability techniques were systematically employed to analyse the internal decision-making mechanisms of each model component. While the predictive accuracy of the deep feature fusion technique demonstrates its effectiveness, understanding why the model performs well is essential, particularly in engineering applications where trust and physical validity are critical.

The deep feature fusion comprises two distinct branches, a statistical ANN and a feature-driven MARCNN, each leveraging different input modalities and learning representations. To interpret the contribution of input features in the ANN branch, SHAP (SHapley Additive exPlanations) analysis was conducted. This method provides model-aware, game-theoretic attributions that quantify the marginal contribution of each input variable to the output prediction, based on the mean force features from the polishing process. In contrast, the MARCNN branch, which processes segmented multi-domain time-series inputs (TD, FD, DWT, and slurry-related features), was analysed using Grad-CAM (Gradient-weighted Class Activation Mapping). Grad-CAM is a visual explanation technique that identifies spatial or temporal regions within input representations that most influence the model's output, thereby offering interpretability at the feature map level.

This section presents a structured explainability analysis for the following three configurations:

1. The ANN branch trained on mean force features.
2. The MARCNN branch without slurry-related pH and temperature features.
3. The MARCNN branch with the inclusion of pH and temperature inputs.

Through this multi-perspective analysis, the objective is to validate whether the learned patterns correspond with domain knowledge of the bonnet polishing process and to identify latent interactions not easily observable via traditional statistical analysis.

7.4.1 XAI for the ANN Branch via SHAP

To unwind the decision-making process within the Artificial Neural Network (ANN) branch of the deep feature fusion network, SHAP analysis was performed. This method provides a theoretically grounded framework rooted in cooperative game theory to quantify the individual contribution of each input feature to the model's output. In this case, the ANN was trained exclusively on statistical features, specifically the mean values of the six force components recorded during polishing. These inputs encapsulate the cumulative force behaviour over each segment, offering a compact yet informative representation of the polishing dynamics. The rationale for using SHAP lies in its ability to attribute prediction outcomes to individual features in a consistent and additive manner. Unlike simple correlation metrics, SHAP values take into account the interactions among features and how they combine non-linearly to influence the model's predictions. This makes SHAP particularly valuable for interpreting deep learning models, which often act as "black boxes."

Figure 7.6 presents the mean absolute SHAP values for each feature, effectively ranking their overall importance. Notably, the Z3 sensor emerged as the most influential input, followed by the X-axis and Z2 force components. This suggests that forces exerted along the vertical axis, typically associated with the normal contact between the bonnet tool and the workpiece, play a critical role in governing material removal. The significance of the X-axis force further emphasizes the influence of lateral frictional forces, which contribute to the energy dissipation and abrasive interactions within the contact zone. In contrast, features such as Y1 and Y2, which correspond to friction/drag force components along the less mechanically engaged direction, contributed relatively less to the prediction.

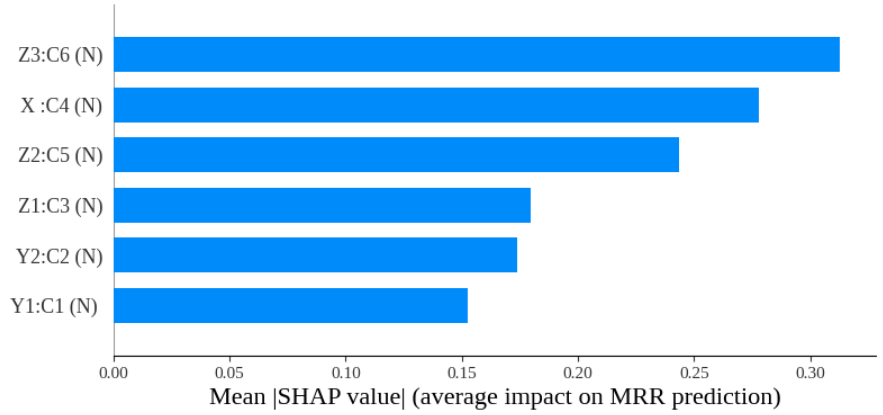

FIGURE 7.6: Mean absolute SHAP values for ANN input features (mean forces). Z3, X, and Z2 show the highest contribution to MRR prediction.

The SHAP summary plot in Fig. 7.7 provides further insights by showing not only the importance of each feature but also the direction and effect size of feature values on the predicted MRR. The clustering of red points (representing higher feature values) towards high positive SHAP values, particularly for Z3 and X, confirms that larger normal and lateral forces generally correspond to higher predicted material removal rates. Conversely, blue points (representing lower input values) cluster toward lower SHAP values, indicating lower predicted outputs. This reveals that the ANN model has learned a physically consistent mapping between force magnitude and material removal response, in line with fundamental polishing principles.

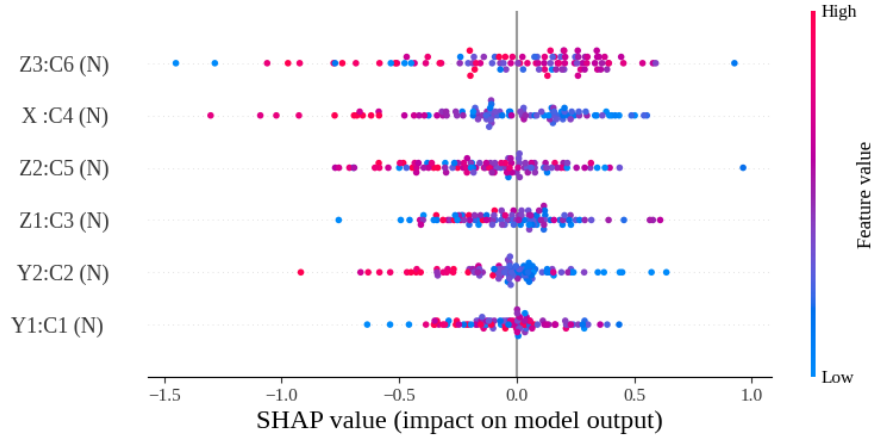

FIGURE 7.7: SHAP summary plot for ANN model inputs. High force values from Z3 and X-axis sensors contribute positively to predicted MRR.

An interesting and informative divergence appears when comparing SHAP results

with traditional distance correlation metrics. For instance, although the Z3 feature did not exhibit the highest linear correlation with MRR as discussed in the previous chapters, it was identified as the most influential under SHAP analysis. This discrepancy indicates the presence of non-linear relationships or feature interactions that are only captured when the full learning dynamics of the model are considered. In this way, SHAP reveals not just associations, but causally-relevant input contributions, which is critical for validating the physical plausibility of learned models.

In practical terms, this explainability analysis has important implications. It assures that the ANN branch is not arbitrarily learning statistical noise, but rather is selectively attending to features that have clear mechanical relevance to the polishing process. The model identifies those force components that represent meaningful physical interactions, namely, the magnitude and direction of applied contact forces, as key indicators of the rate at which material is removed.

The SHAP-based interpretation confirms that the ANN branch of the deep feature fusion network successfully learns intuitive, physics-aligned relationships between sensor-derived force features and the target output (MRR). In addition, it demonstrates the utility of integrating explainability tools in data-driven manufacturing research, providing model transparency, trustworthiness, and diagnostic insight, especially crucial in applications where prediction fidelity and domain knowledge must go hand in hand.

7.4.2 XAI for the MARCNN Branch via Grad-Cam (Without pH and Temperature)

To gain a deeper understanding of how the MARCNN (Multi-branch Attention-Residual CNN) model processes domain-specific features and allocates relevance to different signal representations, Gradient-weighted Class Activation Mapping (Grad-CAM) was applied to its internal convolutional branches. This explainability method allows us to visualize which feature domains, time-domain (TD),

frequency-domain (FD), or discrete wavelet transform (DWT), contribute most significantly to the model's output prediction for each test instance.

Importantly, this analysis was performed using only the force signal-based features, deliberately excluding the slurry-related parameters (pH and temperature). This choice was guided by a key empirical observation: the highest performance metrics were obtained from the MARCNN model when only force features were used, without the inclusion of pH and temperature.

Although slurry properties are physically relevant to material removal, their effect on the model's predictive accuracy was found to be modestly marginal in this dataset. This indicates that the force signals alone capture the dominant dynamics of the polishing process, and hence are sufficient for both accurate prediction and meaningful interpretability.

The resulting Grad-CAM heat-maps, shown in Fig. 7.8, illustrate the activation intensity of each feature branch for three representative predictions. Colour gradients range from blue (lowest relevance) to red (highest relevance), revealing the degree of attention each domain-specific feature set receives.

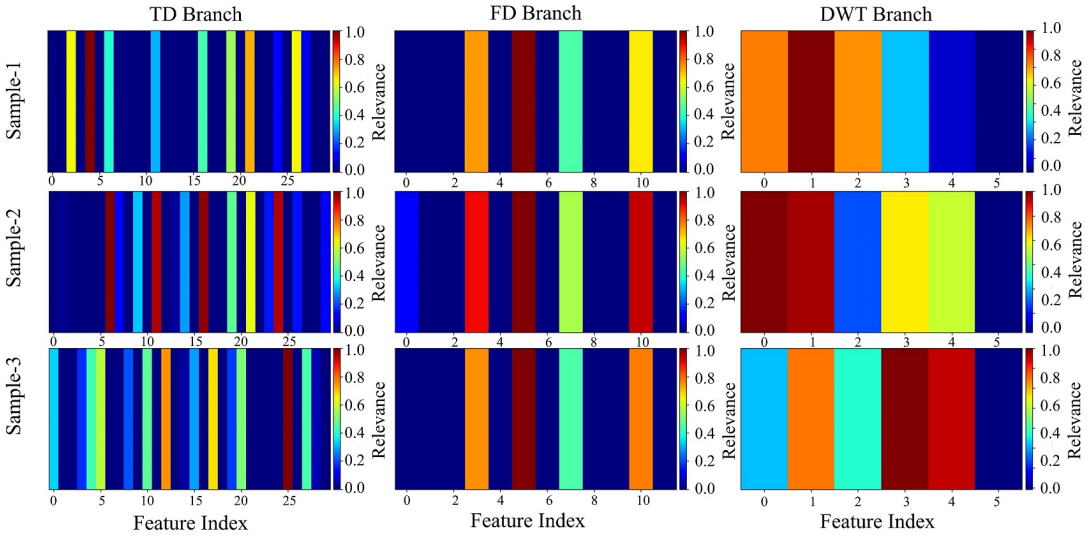

FIGURE 7.8: Grad-CAM heat-maps showing branch-level feature activations for three CNN predictions. Colour intensity reflects the relative importance of TD, FD, and DWT features for each sample.

7.4.3 Sample-Level Interpretations

Sample 1 shows an even distribution of activation across all three branches, suggesting that TD, FD, and DWT features jointly contributed to the prediction. This indicates that the polishing behaviour in this sample was well-characterized by a balanced mix of statistical, spectral, and transient signal attributes—consistent with steady-state or uniformly varying process conditions.

Sample 2 exhibits stronger activations in the FD and DWT branches, implying a greater emphasis on spectral and localized time-frequency information. Such a pattern may arise under polishing conditions where force signals contain oscillatory behaviour, possibly due to machine-tool interactions, surface waviness, or tool wear effects.

Sample 3 demonstrates dominant activation in the DWT branch, indicating that the model relied primarily on wavelet-based features for this case. This likely reflects the presence of subtle, short-duration transients or localized disturbances in the signal, which are well-captured by the DWT representation. The minimal use of TD or FD features here suggests that traditional statistical summaries or global spectral energy were insufficient to explain the underlying process dynamics.

This explainability analysis reinforces the architectural motivation behind MAR-CNN: to process force signal data across complementary domains, each revealing different aspects of polishing behaviour. The model's ability to dynamically shift attention among these domains indicates a form of adaptive learning that reflects the non-stationary and multi-scale nature of the material removal process.

Moreover, the deliberate exclusion of slurry-related features in this analysis serves to highlight the self-sufficiency and informativeness of force data. While pH and temperature are known to influence chemical-mechanical interactions, their relatively small marginal gain in prediction accuracy, observed during controlled ablation studies, suggests that their contribution is secondary when compared to the mechanical force profiles.

Therefore, focusing the interpretability study on force-based features not only provides a clearer window into the model's physical understanding but also aligns with the engineering reality that tool-workpiece interaction forces are the most direct indicators of removal activity.

To sum up, the MARCNN model demonstrates the ability to intelligently parse and prioritize signal domains according to the polishing context. The Grad-CAM visualizations offer strong evidence that the model's internal focus aligns with physical intuition and that force-based features alone are highly sufficient for both accurate prediction and meaningful explanation in the context of MRR forecasting.

7.5 Ablation Study: Evaluating the Impact of pH and Temperature in MARCNN

This section presents an ablation study conducted to evaluate the influence of two key environmental process parameters, slurry pH and temperature, on the predictive performance of the proposed MARCNN model. These variables, although secondary to mechanical forces in the polishing process, are known to affect chemical activity and surface reactivity.

To examine their contribution, the MARCNN model was tested in two configurations: one using only force-derived features (Time-Domain, Frequency-Domain, and DWT), and the other incorporating a fourth input branch comprising pH and temperature.

Table 7.3: Ablation study results for MARCNN: with vs. without pH and temperature input

Configuration	**MAE (μm)**	**R^2 Score**	**RMSE**
Without pH & Temp Data	0.0680	0.9772	0.1719
With pH & Temp Data	0.0691	0.9787	0.1659
Percentage Change	+1.5% (↑)	+0.15% (↑)	−3.49% (↓)

7.5.1 Experimental Setup and Comparison Metrics

In both configurations, the MARCNN architecture maintained identical convolutional and attention mechanisms for the three force-related branches. While the version with environmental parameters added a shallow feed-forward branch for the pH and temperature features. Table 7.3 compares the performance metrics, MAE, R^2, and RMSE, of both configurations over 10 experimental runs.

7.5.2 Observations and Interpretation

The results in Table 7.3 reveal a nuanced picture. While the inclusion of pH and temperature led to a slight improvement in R^2 (by 0.15%) and RMSE (by 3.49%), the Mean Absolute Error (MAE) increased by 1.5%. This suggests that while the model may have captured slightly more variance in the data and reduced the impact of outliers, its average pointwise accuracy deteriorated. The inconsistency across evaluation metrics implies that pH and temperature data, though theoretically meaningful, contributed marginally and not uniformly to prediction quality. This behaviour can be interpreted in light of the physical nature of the polishing process. Force signals, especially those aligned with the Z-axis and X-axis, directly capture the mechanical interactions at the polishing interface and therefore hold primary explanatory power for material removal. In contrast, slurry pH and temperature influence material removal through slower chemical and thermal effects, which are both indirect and subtle in nature. Furthermore, their values exhibited low temporal and spatial variance across polishing runs, limiting their information content for learning-based models.

7.5.3 Architectural and Learning Considerations

From a deep learning perspective, the environmental input branch in the MARCNN was relatively shallow compared to the force-feature branches equipped with convolutional and attention layers. This structural asymmetry likely caused the environmental pathway to receive less back-propagated signal during training.

Moreover, due to the model's inherent optimization behaviour, branches with higher gradient flow (typically the force branches) naturally dominate learning unless strong regularization or fusion is applied.

Additionally, it is plausible that some of the statistical effects of slurry pH and temperature, such as their influence on slurry reactivity or tool-workpiece lubrication, were already reflected in variations in the force signal itself. As a result, the environmental features may have provided redundant information, adding complexity without yielding substantial new learning.

7.5.4 Supporting Evidence from Explainability Analysis

This interpretation is further corroborated by the Grad-CAM-based branch-wise activation plot shown in Fig. 7.9. While earlier visualizations (e.g., Fig. 7.8) captured attention across different branches for individual predictions, the plot below aggregates the relative activation strength across all feature indices within each input stream: time-domain (TD), frequency-domain (FD), discrete wavelet transform (DWT), and the pH/temperature inputs.

As shown in Fig. 7.9, the TD, FD, and DWT branches exhibit high and spatially distributed activation values, confirming their substantial involvement in the model's decision process. In contrast, the pH and temperature branch shows no activation for this sample and partial activation for some cases, with features barely activated and a showing mild responses. This pattern indicates that while these process parameters are not entirely ignored, they contribute far less to the predictive logic of the model.

The limited activation suggests that the pH and temperature features likely encode low-salience or redundant information, especially when compared to the rich temporal and spectral structure captured from force data. Their weaker influence may stem from lower variance, indirect correlation with material removal, or insufficient signal strength for the model to learn robust associations during training.

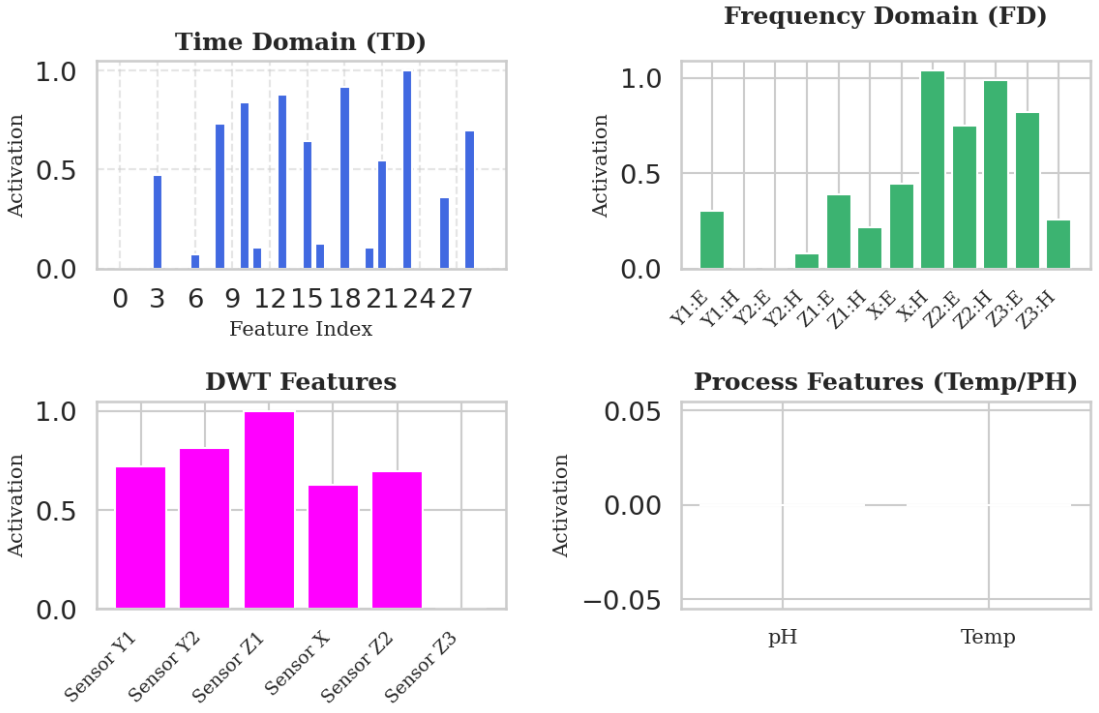

FIGURE 7.9: Grad-CAM activation magnitudes across feature indices for all MARCNN input branches for a sample prediction. Strong activations are observed for TD, FD, and DWT features, whereas the PH and Temp branch shows no activations.

These activation trends support the conclusion drawn from the ablation study results that the inclusion of pH and temperature yields negligible improvement and may even introduce mild inconsistency. Thus, the decision to prioritize process force features in final model explainability and deployment is empirically justified.

Overall, the ablation study demonstrates that while pH and temperature are relevant from a theoretical standpoint, their stand-alone inclusion within the current architecture does not significantly enhance the model's predictive capability.

Future studies may consider more advanced fusion strategies, temporal derivatives of environmental variables, or attention-based cross-branch learning mechanisms to better leverage this data. For the current model and dataset, however, the core predictive power lies predominantly in the mechanical force features.

7.6 Evaluation of Predictive Gain vs. Computational Cost

The quantitative improvement in predictive accuracy may seem modest at first glance, but it holds substantial practical value in high-precision polishing applications. The Mean Absolute Error (MAE) reduced from 0.0713 µm in the baseline ANN model to 0.0563 µm in the proposed deep feature fusion network with a relative decrease of approximately 15 nm or 21%. Similarly, the Root Mean Squared Error (RMSE) improved from 0.1373 µm to 0.1239 µm, while the R^2 score increased from 0.9854 to 0.9881. In the context of ultra-precision surface finishing, where tolerances are often within sub-micron or nanometre levels, even small improvements in prediction accuracy can result in significant downstream benefits. For instance, during batch polishing operations across 50–100 runs, a per-run error reduction of 15 nm translates to a cumulative error avoidance of 0.75–1.5 µm. This level of magnitude is sufficient to prevent rework, reduce over-polishing, or eliminate the need for corrective processing. These improvements help ensure that the workpiece remains within acceptable surface deviation limits and contribute to reduced cycle time and less material waste.

The cost of achieving this improvement, from a computational standpoint, is carefully managed and largely concentrated in the training phase. The deep feature fusion, which integrates an MARCNN with an ANN feature stream, requires more computational resources than a stand-alone ANN. Model training and evaluation were conducted on a cloud-based platform equipped with an NVIDIA L4 GPU (24 GB VRAM), supported by 2–4 virtual CPUs and approximately 52 GB of system RAM. The deep feature fusion architecture, while introducing additional computational complexity compared to baseline models, remained computationally feasible and was optimized to complete within a reasonable training time. The marginal increase in training time is balanced by the improvement in prediction performance. The sizes of these models are given below: The ANN model is lightweight at 179 KB. The MARCNN branch alone is 155.6 MB. The final deep feature fusion network amounts to 259.5 MB. The inference time for deep feature

fusion network remains efficient, with processing times of 70 ms per input sample, supporting a near real-time implementation. In near real-time or closed-loop polishing setups, this latency is negligible and compatible with industrial cycle times. While the improvements in performance metrics may appear modest in isolation, their cumulative impact over time, especially across repeated operations, can justify the one-time training cost. These gains contribute meaningfully to enhancing process efficiency and predictive modelling accuracy.

To summarize this chapter, it can be concluded that the proposed deep feature fusion strategy, comprising an ANN branch for statistical features and an MARCNN branch for multi-domain time series inputs, demonstrated superior predictive performance for estimating MRR in bonnet polishing. It consistently outperformed stand-alone ANN and CNN models in terms of MAE, RMSE, and R^2, validating the complementary strengths of statistical and temporal representations. Diagnostic plots further confirmed that the deep feature fusion strategy maintained low prediction bias and well-behaved residuals, indicating stable and generalizable behaviour across diverse polishing conditions.

Explainability analyses revealed that vertical (Z-axis) and lateral (X-axis) forces were the most influential in the ANN branch, while Grad-CAM visualizations showed that the MARCNN model dynamically distributed attention across TD, FD, and DWT features. Ablation results indicated that the addition of pH and temperature data offered limited benefit and, in some cases, introduced inconsistency, suggesting that force-based features remain the dominant drivers of predictive accuracy. Collectively, these results underscore the effectiveness and interpretability of the proposed deep feature fusion approach for data-driven modelling in precision polishing.

Chapter 8

Conclusion and Future Work

Conclusion

This study presented a comprehensive data-driven framework for predicting Material Removal Rate (MRR) in bonnet polishing of optical surfaces using multi-sensor time-series data. Recognizing the limitations of conventional physical models, such as Preston's equation, in capturing the complex, non-linear behaviour of modern polishing systems, this work adopted a machine learning perspective grounded in rigorous data preprocessing, domain-specific feature extraction, and model interpretability.

A robust preprocessing pipeline was designed to address the inherent noise and variability in force sensor data. This pipeline used K-means clustering to automatically identify and exclude non-polishing segments, followed by systematic segmentation of polishing intervals into equal steps. From each segment, features were extracted in multiple domains: time-domain statistics, frequency-domain measures, and wavelet-based representations. Additionally, environmental process parameters, slurry pH and temperature, were incorporated to explore their supplementary predictive value.

The predictive modelling strategy was centred around a hybrid deep feature fusion architecture. The deep feature fusion combined an Artificial Neural Network

(ANN), trained on mean force features, with a Multi-Branch Attention Residual Convolutional Neural Network (MARCNN), trained on domain-transformed time-series inputs (TD, FD, and DWT). Each branch of MARCNN processed a specific signal representation, capturing localized temporal patterns and high-frequency behaviours that statistical features alone could not.

Together, the ANN and MARCNN branches fed into a fusion layer to predict MRR. Performance evaluation showed that the deep feature fusion architecture achieved superior predictive capability across multiple metrics, including a mean absolute error of 0.0563 μm and an R^2 score of 0.9881. Compared to individual models, ANN and MARCNN alone, the deep feature fusion consistently outperformed both, validating the hypothesis that fusing statistical and temporal feature pathways leads to more accurate and reliable predictions. Diagnostic visualizations, including actual vs. predicted plots and residual histograms, further confirmed the model's robustness, with errors displaying normality and no systemic bias.

Explainable AI techniques were applied to provide transparency into model behaviour. SHAP analysis for the ANN branch revealed that the vertical (Z-axis) and lateral (X-axis) forces had the highest impact on MRR prediction, aligning well with physical expectations from contact mechanics. Grad-CAM visualizations of the MARCNN model revealed sample-specific attention distributions across time, frequency, and wavelet domains, offering insights into how the model weighs different signal features during prediction.

An ablation study revealed that while pH and temperature are theoretically relevant, their inclusion had minimal impact on performance suggesting either weak correlation with MRR or redundancy in the force signals. Overall, this work contributes a reproducible, interpretable, and highly accurate predictive framework for MRR estimation in precision polishing. It moves beyond black-box modelling by combining engineered features with explainability, and lays a solid foundation for real-time process monitoring, quality control, and future integration into smart manufacturing environments.

Future Work

This work lays the foundation for intelligent data-driven prediction of MRR in bonnet polishing using multi-domain sensor inputs. Building on the demonstrated potential of the current deep feature fusion network, future work will explore several key directions to both deepen scientific understanding and improve practical deployment capabilities.

Firstly, the integration of transformer-based models, which are well-suited for capturing long-range dependencies and complex temporal dynamics, presents a compelling opportunity to improve upon the CNN's performance, especially in modelling temporal variations in force signals. In parallel, additional process-specific features, such as slurry particle size distribution will be incorporated to capture the abrasive characteristics of the polishing medium, which are known to influence MRR but were not fully exploited in the current study.

Furthermore, the current dataset is spatially limited, as MRR measurements were collected from a narrow central strip of the workpiece. To address this limitation, future work will involve synthetic data generation and augmentation, aimed at simulating polishing across varied spatial zones. This would enable the development of a model capable of predicting spatially distributed MRR patterns, enhancing generalizability and usability for surface shape control.

Finally, to enable real-time monitoring and edge deployment in industrial environments, the model will be optimized for resource-constrained hardware platforms. This will involve applying quantization, pruning, and compression techniques to reduce model size and inference latency, while maintaining predictive accuracy. Such advancements would pave the way for in-situ implementation on polishing platforms, supporting adaptive process control and smart manufacturing.

Bibliography

[1] W. Grzesik, "Influence of surface textures produced by finishing operations on their functional properties," *Journal of Machine Engineering*, vol. 16, no. 1, pp. 15–23, 2016.

[2] M. Xie, Y. Pan, Z. An, S. Huang, and M. Dong, "Review on surface polishing methods of optical parts," *Advances in Materials Science and Engineering*, vol. 2022, no. 1, p. 8723269, 2022.

[3] E. Rabinowicz, "Polishing," *Scientific American*, vol. 218, no. 6, pp. 91–101, 1968.

[4] Z. Luo, Z. Zhang, F. Zhao, C. Fan, J. Feng, H. Zhou, F. Meng, X. Zhuang, and J. Wang, "Advanced polishing methods for atomic-scale surfaces: A review," *Materials Today Sustainability*, p. 100841, 2024.

[5] C. J. Evans, E. Paul, D. Dornfeld, D. A. Lucca, G. Byrne, M. Tricard, F. Klocke, O. Dambon, and B. A. Mullany, "Material removal mechanisms in lapping and polishing," *CIRP annals*, vol. 52, no. 2, pp. 611–633, 2003.

[6] B. Tuck, "The chemical polishing of semiconductors," *Journal of Materials Science*, vol. 10, pp. 321–339, 1975.

[7] M. Kumar, A. Kumar, H. Yadav, A. Alok, and M. Das, "Abrasive based finishing method applied on biomedical implants: A review," *Materials Today: Proceedings*, vol. 47, pp. 3985–3992, 2021.

[8] Z.-W. Zhong, "Advanced polishing, grinding and finishing processes for various manufacturing applications: a review," *Materials and Manufacturing Processes*, vol. 35, no. 12, pp. 1279–1303, 2020.

[9] M. Kumar, H. N. Singh Yadav, A. Kumar, and M. Das, "An overview of magnetorheological polishing fluid applied in nano-finishing of components," *Journal of Micromanufacturing*, vol. 5, no. 2, pp. 82–100, 2022.

[10] Z. Zhong, "Recent advances in polishing of advanced materials," *Materials and Manufacturing Processes*, vol. 23, no. 5, pp. 449–456, 2008.

[11] S. Rebeggiani and B.-G. Rosén, "A step-by-step analysis of manual polishing sequences," in *Tool 2012-The 9th International Tooling Conference, 11-14 September, 2012, Leoben, Austria*, 2012, pp. 317–324.

[12] K. B. Wang, F. Dailami, and J. Matthews, "Towards collaborative robotic polishing of mould and die sets," *Procedia Manufacturing*, vol. 38, pp. 1499–1507, 2019.

[13] D. Zhao and X. Lu, "Chemical mechanical polishing: theory and experiment," *Friction*, vol. 1, pp. 306–326, 2013.

[14] Z. Geng, N. Huang, M. Castelli, and F. Fang, "Polishing approaches at atomic and close-to-atomic scale," *Micromachines*, vol. 14, no. 2, p. 343, 2023.

[15] M.-M. Lu, Y.-K. Yang, J.-Q. Lin, Y.-S. Du, and X.-Q. Zhou, "Research progress of magnetorheological polishing technology: a review," *Advances in Manufacturing*, pp. 1–37, 2024.

[16] D. Golini, W. I. Kordonski, P. Dumas, and S. J. Hogan, "Magnetorheological finishing (mrf) in commercial precision optics manufacturing," in *Optical manufacturing and testing III*, vol. 3782. SPIE, 1999, pp. 80–91.

[17] H. Sun, X. Zhao, and J. Yin, "Progress in the study of electrorheological polishing: A review," *Journal of Intelligent Material Systems and Structures*, vol. 34, no. 17, pp. 1961–1982, 2023.

[18] X. Liu, J. Wang, D. Teng, P. J. Liew, and C. Huang, "Electrorheological fluid–assisted ultrasonic polishing for in625 additively manufactured surfaces," *The International Journal of Advanced Manufacturing Technology*, vol. 120, no. 1, pp. 891–905, 2022.

[19] Z. Wu, J. Shen, Y. Peng, and X. Wu, "Review on ultra-precision bonnet polishing technology," *The International Journal of Advanced Manufacturing Technology*, vol. 121, no. 5, pp. 2901–2921, 2022.

[20] D. D. Walker, A. Beaucamp, D. Brooks, R. Freeman, A. King, G. McCavana, R. Morton, D. Riley, and J. Simms, "Novel cnc polishing process for control of form and texture on aspheric surfaces," in *Current Developments in Lens Design and Optical Engineering III*, vol. 4767. SPIE, 2002, pp. 99–105.

[21] X. Su, P. Ji, K. Liu, D. Walker, G. Yu, H. Li, D. Li, and B. Wang, "Combined processing chain for freeform optics based on atmospheric pressure plasma processing and bonnet polishing," *Optics Express*, vol. 27, no. 13, pp. 17 979–17 992, 2019.

[22] S. Zeng and L. Blunt, "Experimental investigation and analytical modelling of the effects of process parameters on material removal rate for bonnet polishing of cobalt chrome alloy," *Precision Engineering*, vol. 38, no. 2, pp. 348–355, 2014.

[23] F. Preston, "The theory and design of plate glass polishing machines," *J. Society of glass Tech.*, vol. 11, p. 214, 1927.

[24] Y. Lu, X. Xu, and L. Wang, "Smart manufacturing process and system automation–a critical review of the standards and envisioned scenarios," *Journal of Manufacturing Systems*, vol. 56, pp. 312–325, 2020.

[25] F. Tao, Q. Qi, A. Liu, and A. Kusiak, "Data-driven smart manufacturing," *Journal of manufacturing systems*, vol. 48, pp. 157–169, 2018.

[26] J. Yuan, B. Lyu, W. Hang, and Q. Deng, "Review on the progress of ultra-precision machining technologies," *Frontiers of mechanical engineering*, vol. 12, pp. 158–180, 2017.

[27] Z. Jurkovic, G. Cukor, M. Brezocnik, and T. Brajkovic, "A comparison of machine learning methods for cutting parameters prediction in high speed turning process," *Journal of Intelligent Manufacturing*, vol. 29, no. 8, pp. 1683–1693, 2018.

[28] J. Peng, W. Sun, J. Xu, G. Zhou, L. Xie, H. Han, Y. Xiao, J. Chen, and Q. Li, "Analyzing process parameters for industrial grinding circuit based on machine learning method," *Advanced Powder Technology*, vol. 34, no. 9, p. 104113, 2023.

[29] M. Schneckenburger, L. Garcia-Barth, and R. Börret, "Machine learning model for robot polishing cell," in *Seventh European Seminar on Precision Optics Manufacturing*, vol. 11478. SPIE, 2020, pp. 145–154.

[30] P. Yunfeng, H. Jiakuan, H. Xuepeng, L. Jiaming, W. Zhenzhong, L. Chenlei, and W. Jinghang, "Ultra-precision grinding and polishing processing technology research and equipment development," *Opto-Electronic Engineering*, vol. 50, no. 4, pp. 220 097–1, 2023.

[31] Z. Wang, C. Shi, P. Zhang, Z. Yang, Y. Chen, and J. Guo, "Recent progress of advanced optical manufacturing technology," *Journal of mechanical engineering*, vol. 57, no. 8, pp. 23–56, 2021.

[32] B. Zhong, C. Wang, X. Chen, and J. Wang, "Time-varying tool influence function model of bonnet polishing for aspheric surfaces," *Applied Optics*, vol. 58, no. 4, pp. 1101–1109, 2019.

[33] M. Darowski, M. F. Aftab, H. Li, D. Walker, G. Yu, C. An, and C. W. Omlin, "Towards data-driven material removal rate estimation in bonnet polishing," in *2023 11th International Conference on Control, Mechatronics and Automation (ICCMA)*. IEEE, 2023, pp. 473–479.

[34] A. Cordero-Dávila, R. Izazaga-Pérez, J. González-García, and J. Cuautle-Cortés, "Polisher density into preston equation," *Optik*, vol. 124, no. 19, pp. 3909–3912, 2013.

[35] L. Téllez-Arriaga, A. Cordero-Dávila, C. I. Robledo-Sánchez, and J. Cuautle-Cortés, "Correction of the preston equation for low speeds," *Applied optics*, vol. 46, no. 9, pp. 1408–1410, 2007.

[36] Q. Luo, S. Ramarajan, and S. Babu, "Modification of the preston equation for the chemical–mechanical polishing of copper," *Thin solid films*, vol. 335, no. 1-2, pp. 160–167, 1998.

[37] E. Luna-Aguilar, A. Cordero-Davila, J. Gonzalez, M. Nunez-Alfonso, V. Cabrera, C. I. Robledo-Sanchez, J. Cuautle-Cortez, and M. H. Pedrayes, "Edge effects with the preston equation," in *Future giant telescopes*, vol. 4840. SPIE, 2003, pp. 598–603.

[38] C. Shi, Y. Peng, L. Hou, Z. Wang, and Y. Guo, "Improved analysis model for material removal mechanisms of bonnet polishing incorporating the pad wear effect," *Applied optics*, vol. 57, no. 25, pp. 7172–7186, 2018.

[39] T. Suratwala, J. Menapace, R. Steele, L. Wong, G. Tham, N. Ray, B. Bauman, M. Gregory, and T. Hordin, "Mechanisms influencing and prediction of tool influence function spots during hemispherical sub-aperture tool polishing on fused silica," *Applied Optics*, vol. 60, no. 1, pp. 201–214, 2020.

[40] C. Shi, Y. Peng, L. Hou, Z. Wang, and Y. Guo, "Micro-analysis model for material removal mechanisms of bonnet polishing," *Applied optics*, vol. 57, no. 11, pp. 2861–2872, 2018.

[41] J. Zhang, Y. Jiang, H. Luo, and S. Yin, "Prediction of material removal rate in chemical mechanical polishing via residual convolutional neural network," *Control Engineering Practice*, vol. 107, p. 104673, 2021.

[42] H. Liang, W. Chen, Y. Fu, W. Zhou, L. Mo, Y. Jian, Q. Wen, D. Liu, and J. He, "Back propagation neural network-based predictive model for magnetorheological–chemical polishing of silicon carbide," *Micromachines*, vol. 16, no. 3, p. 271, 2025.

[43] T. Yu, Z. Li, and D. Wu, "Predictive modeling of material removal rate in chemical mechanical planarization with physics-informed machine learning," *Wear*, vol. 426, pp. 1430–1438, 2019.

[44] R. Wang, C. F. Cheung, Y. Zang, C. Wang, and C. Liu, "Material removal rate optimization with bayesian optimized differential evolution based on deep

learning in robotic polishing," *Journal of Manufacturing Systems*, vol. 78, pp. 178–186, 2025.

[45] R. Pan, W. Zhao, B. Zhong, D. Chen, Z. Wang, C. Zha, and J. Fan, "Evaluation of removal characteristics of bonnet polishing tool using polishing forces collected online," *Journal of Manufacturing Processes*, vol. 47, pp. 393–401, 2019.

[46] F. Tian, C. Lv, Z. Li, and G. Liu, "Modeling and control of robotic automatic polishing for curved surfaces," *CIRP Journal of Manufacturing Science and Technology*, vol. 14, pp. 55–64, 2016.

[47] C. Miao, J. C. Lambropoulos, and S. D. Jacobs, "Process parameter effects on material removal in magnetorheological finishing of borosilicate glass," *Applied optics*, vol. 49, no. 10, pp. 1951–1963, 2010.

[48] Y. Homma, K. Fukushima, S. Kondo, and N. Sakuma, "Effects of mechanical parameters on cmp characteristics analyzed by two-dimensional frictional-force measurement," *Journal of The Electrochemical Society*, vol. 150, no. 12, p. G751, 2003.

[49] J. Jeong, Y. Shin, S. Jeong, S. Jeong, and H. Jeong, "Deep ensemble learning for material removal rate prediction in chemical mechanical planarization with pad surface topography," *Precision Engineering*, vol. 88, pp. 777–787, 2024.

[50] Z. Li, D. Wu, and T. Yu, "Prediction of material removal rate for chemical mechanical planarization using decision tree-based ensemble learning," *Journal of Manufacturing Science and Engineering*, vol. 141, no. 3, p. 031003, 2019.

[51] M. Schneckenburger, S. Höfler, L. Garcia, R. Almeida, and R. Börret, "Material removal predictions in the robot glass polishing process using machine learning," *SN Applied Sciences*, vol. 4, no. 1, p. 33, 2022.

[52] C.-L. Liu, C.-J. Tseng, W.-H. Hsaio, S.-H. Wu, and S.-R. Lu, "Predicting the wafer material removal rate for semiconductor chemical mechanical polishing using a fusion network," *Applied Sciences*, vol. 12, no. 22, p. 11478, 2022.

[53] J. Deng, Q. Zhang, J. Lu, Q. Yan, J. Pan, and R. Chen, "Prediction of the surface roughness and material removal rate in chemical mechanical polishing of single-crystal sic via a back-propagation neural network," *Precision Engineering*, vol. 72, pp. 102–110, 2021.

[54] P. Wang, R. X. Gao, and R. Yan, "A deep learning-based approach to material removal rate prediction in polishing," *CIRP annals*, vol. 66, no. 1, pp. 429–432, 2017.

[55] G. Wang, H. Sun, R. Wu, Q. Liu, and Q. Liu, "A deep belief network model for predicting the material removal rate in the polishing process," *Proceedings of the Institution of Mechanical Engineers, Part E: Journal of Process Mechanical Engineering*, p. 09544089241282439, 2024.

[56] Y. Wei and D. Wu, "Material removal rate prediction in chemical mechanical planarization with conditional probabilistic autoencoder and stacking ensemble learning," *Journal of Intelligent Manufacturing*, vol. 35, no. 1, pp. 115–127, 2024.

[57] Z. Song, W. Zhao, X. Zhang, M. Ke, W. Fang, and B. Lyu, "Stacking ensemble learning based material removal rate prediction model for cmp process of semiconductor wafer," *AI EDAM*, vol. 38, p. e17, 2024.

[58] S. Saravanakumar, S. Sathiyamurthy, and V. Vinoth, "Enhancing machining accuracy of banana fiber-reinforced composites with ensemble machine learning," *Measurement*, vol. 235, p. 114912, 2024.

[59] V. Warke, S. Kumar, A. Bongale, and K. Kotecha, "Robust tool wear prediction using multi-sensor fusion and time-domain features for the milling process using instance-based domain adaptation," *Knowledge-Based Systems*, vol. 288, p. 111454, 2024.

[60] Y. Xue, C. Wen, Z. Wang, W. Liu, and G. Chen, "A novel framework for motor bearing fault diagnosis based on multi-transformation domain and multi-source data," *Knowledge-Based Systems*, vol. 283, p. 111205, 2024.

[61] X. Zhang, C. Krewet, and B. Kuhlenkötter, "Automatic classification of defects on the product surface in grinding and polishing," *International Journal of Machine Tools and Manufacture*, vol. 46, no. 1, pp. 59–69, 2006.

[62] M. Rao, Y. Zhang, H. Wang, H. Ming, Y. Zhao, and J. Zhu, "Towards modeling and restraining surface ripples during bonnet polishing based on frequency domain characteristic control," *CIRP Annals*, vol. 72, no. 1, pp. 493–496, 2023.

[63] A. Li and R. Qi, "Analysis and prediction of contact fault detection in automatic flexible polishing for complex surfaces based on woa-svm," *Industrial Robot: the international journal of robotics research and application*, 2025.

[64] F. Guo, Y. Liu, P. Wang, J. Ma, G. Zhang, J. Han, D. Wang, and L. Yin, "Acoustic emission based classification of processing states for laser polishing," *Lasers in Manufacturing and Materials Processing*, pp. 1–30, 2025.

[65] B. De Agustina, M. M. Marín, R. Teti, and E. M. Rubio, "Analysis of force signals for the estimation of surface roughness during robot-assisted polishing," *Materials*, vol. 11, no. 8, p. 1438, 2018.

[66] M. Darowski, M. F. Aftab, D. Walker, and C. W. Omlin, "Data-driven material removal rate estimation in bonnet polishing process," in *14th IFAC Symposium on Dynamics and Control of Process Systems (DYCOPS 2025)*, 2025.